Russian Geology and Geophysics © 2020, V.S. Sobolev IGM, Siberian Branch of the RAS
Vol. 61, No. 2, pp. 119–138, 2020 *DOI:10.15372/RGG2019087* *Geologiya i Geofizika*

Geochemistry, Sm–Nd, Rb–Sr, and Lu–Hf Isotopes, Sources, and Conditions of Formation of Early Paleozoic Plagiogranitoids in the South of the Lake Zone in Western Mongolia

S.N. Rudnev[a, ✉], V.G. Mal'kovets[a,b,c], E.A. Belousova[d], I.G. Tret'yakova[a,e], P.A. Serov[f], V.Yu. Kiseleva[a], A.A. Gibsher[a,b,c], I.V. Nikolaeva[a]

[a] *V.S. Sobolev Institute of Geology and Mineralogy, Siberian Branch of the Russian Academy of Sciences, pr. Akademika Koptyuga 3, Novosibirsk, 630090, Russia*

[b] *ALROSA Geological Research Enterprise (Public Joint-Stock Company), Chernyshevskoe shosse 16, Mirnyi, Republic of Sakha (Yakutia), 678170, Russia*

[c] *Novosibirsk State University, ul. Pirogova 1, Novosibirsk, 630090, Russia*

[d] *Australian Research Council Centre of Excellence for Core to Crust Fluid Systems / GEMOC, Department of Earth and Planetary Science, Macquarie University, Sydney, NSW 2109, Australia*

[e] *Central Research Geological Prospecting Institute of Nonferrous and Noble Metals, Varshavskoe shosse 129, korp. 1, Moscow, 117545, Russia*

[f] *Institute of Geology, Kola Science Center of the Russian Academy of Sciences, ul. Fersmana 14, Apatity, 184209, Russia*

Received 20 August 2018; received in revised form 21 December 2018; accepted 25 December 2019

Abstract—We present results of geochemical and isotope (Rb–Sr, Sm–Nd, and Lu–Hf) studies of the early Paleozoic plagiogranitoid associations in the south of the Lake Zone in Western Mongolia, which formed at the island-arc and accretion–collision stages of the regional evolution. According to the petrogeochemical composition, the early Paleozoic plagiogranitoid associations of the island-arc (Tugrug, Hatan-Hunga, Udzur-Hunga, and Bayasgalant plutons, 531–517 Ma) and accretion–collision (Tugrug, Mandalt, and Dut Uul plutons, 504–481 Ma) stages are high- and low-alumina rocks. The recognized types of plagiogranitoids, with regard to their trace-element composition, indicate that their parental melts were generated from MORB-type metabasites at ≥10–12 kbar, in equilibrium with garnet-containing restite, and at ≤8 kbar, in equilibrium with plagioclase-containing restite. The Sr–Nd isotope data on the rocks and the Lu–Hf isotope parameters of their magmatic zircons show two groups of plagiogranitoids, with different sources of melts. The first group includes plagiogranitoid associations of most plutons (Tugrug, Udzur-Hunga, Hatan-Hunga, Bayasgalant, and Dut Uul) with isotope parameters (ε_{Nd} = 8.5–4.6, $(^{87}Sr/^{86}Sr)_0$ = 0.7034–0.7036, and ε_{Hf} = 14.7–11.9) indicating the juvenile nature of their sources. The second group includes plagiogranitoids of the Mandalt pluton; their isotope parameters (ε_{Nd} = 1.4–0.2, $(^{87}Sr/^{86}Sr)_0$ = 0.7053, and ε_{Hf} = 7.2–5.4) indicate that the parental melts were generated mostly from enriched-mantle metabasites. The Hf isotope data on inherited and xenogenic zircons (664–519 Ma) from the early Paleozoic plagiogranitoid associations of the southern Lake Zone permit us to separate these rocks into three groups according to their ε_{Hf} values (14.5–12.8, 2.9, and 10.6–6.7). The Hf isotope parameters of magmatic and inherited zircons, with regard to their age, indicate that the source of the parental melts lacked rocks with a long crustal history, such as the early Precambrian associations of the Dzavhan microcontinent.

Keywords: granitoid magmatism, geochemistry, Nd–Sr–Hf isotopy, Central Asian Orogenic Belt, Lake Zone in Western Mongolia

INTRODUCTION

The Lake Zone of the early Caledonides in Western Mongolia is a late Neoproterozoic–early Cambrian island-arc terrane (Dergunov, 1989; Dergunov et al., 2001; Badarch et al., 2002), part of the Caledonian superterrane of the Central Asian Orogenic Belt (CAOB). The Nd isotope data on the late Neoproterozoic and early Cambrian volcanic complexes of the Lake Zone, along with their geologic structure, age, and geochemical features (Jahn et al., 2000a,b; Jahn, 2004; Kovach et al., 2011; Yarmolyuk et al., 2011, 2012) led to the conclusion that the juvenile crust formed from depleted mantle sources in the oceanic island-arc and plateau settings in the late Neoproterozoic–Cambrian (570–490 Ma), with involvement of ancient crustal material (sedi-

✉ Corresponding author.
E-mail address: rudnev@igm.nsc.ru (S.N. Rudnev)

ments) in subduction zones. The subsequent accretion–collision processes involved paleo-oceanic and island-arc complexes and the Precambrian Dzavhan microcontinent.

Late Neoproterozoic–early Paleozoic intrusive rock associations are widespread among island-arc volcanics of the Lake Zone, with granitoids being predominant and gabbroids being subordinate (Fig. 1). These associations formed in island-arc and accretion–collision settings and have different ages (from late Neoproterozoic to Middle–Late Ordovician) and petrogeochemical and isotope characteristics (Kovalenko et al., 2004; Rudnev et al., 2009, 2012, 2016; Yarmolyuk et al., 2011). It was established that gabbroid and granitoid associations in the northern and central parts of the Lake Zone are dated at 551–449 Ma and are characterized by positive ε_{Nd} values (9.0–5.2) and low Sr isotope ratios $((^{87}Sr/^{86}Sr)_0$ = 0.7034–0.7048) (Kovalenko et al., 2004; Rudnev et al., 2009, 2012, 2013; Kovach et al., 2011).

Information about the geologic structure, age, and petrochemical composition of granitoid and gabbroid associations in the south of the Lake Zone (Tuguruk, Tugrug, Udzur-Hunga, Hatan-Hunga, Mandalt, Bayasgalant, and Dut Uul plutons, Fig. 1) is given in more detail in our previous paper (Rudnev et al., 2019). The formation of plagiogranitoids and gabbroids in this segment of the Lake Zone took place at 531 to 481 Ma and was related to two geodynamic stages of the regional evolution: island-arc, 531–517 Ma (Tuguruk, Tugrug, Udzur-Hunga, Hatan-Hunga, and Bayasgalant plutons) and accretion–collision, 504–481 Ma (Tugrug, Mandalt, and Dut Uul plutons). According to the petrochemical composition, the above plagiogranitoid (tonalite–trondjemite) associations belong to the calc-alkalic series and are similar to plagiogranitoids of the northern and central parts of the same belt. Along with magmatic zircons with an age of 531 to 481 Ma, xenogenic and inherited zircons[1] were found in the studied plagiogranitoids (Rudnev et al., 2018, 2019). Four age groups of xenogenic and inherited zircons (~664, 570–560, 545–531, and 530–519 Ma) are recognized; they generally mark the main stages of island-arc (volcanic and intrusive) and ophiolite magmatism and, probably, the magma-generating substrates involved in melting during the formation of plagiogranitoids. The absence of xenogenic and inherited zircons older than 664 Ma from the early Paleozoic plagiogranitoids in the south of the Lake Zone (axial part) suggests the remoteness of the island arc of the Lake Zone from the early Precambrian terranes (Dzavhan microcontinent).

The goal of this research work was to elucidate the conditions of formation of the parental melts and the type of magma-generating sources for the early Paleozoic plagiogranitoid associations in the south of the Lake Zone, which formed during two stages in different geodynamic settings. Based on the earlier geological, geochronological, and petrochemical studies (Rudnev et al., 2019), we obtained new data on the geochemistry and isotope (Sm–Nd and Sr–Nd) composition of plagiogranitoid associations in the south of the Lake Zone (Tugrug, Udzur-Hunga, Hatan-Hunga, Mandalt, Bayasgalant, and Dut Uul plutons) and on the Hf isotope composition of zircon generations of different ages. The information obtained makes it possible to determine not only the formation conditions of the parental melts of these plagiogranitoids but also their magma-generating sources. Using the Hf isotope characteristics of magmatic, xenogenic, and inherited zircons also permits evaluation of the contribution of ancient crustal substrates to the genesis of granitoids at different geodynamic stages of the regional evolution.

METHODS

The contents of major components were determined by XRF at the Analytical Center for Multi-Elemental and Isotope Research, SB RAS, Novosibirsk, using an SRM-25 spectrometer (analysts N.G. Karmanova and A.N. Toryanik). The contents of trace and rare-earth elements were measured by ICP MS on a Finnigan Element mass spectrometer at the same analytical center, following the technique by Nikolaeva et al. (2008); the errors of their determination were <10%.

Sm–Nd isotope studies of bulk samples were carried out on a Finnigan MAT-262 (RPQ) mass spectrometer at the Geological Institute of the Kola Science Center, Apatity. The Nd isotope ratios were normalized to the value $^{146}Nd/^{144}Nd$ = 0.7219. The error of determination of $^{147}Sm/^{144}Nd$ was 0.3% (2σ). The blank contained 0.06 ng Sm and 0.3 ng Nd. The average $^{143}Nd/^{144}Nd$ value in the JNd$_i$-1 standard during the measurements was 0.512090 ± 13 (N = 15). The values of $\varepsilon_{Nd}(T)$ were calculated using modern chondrite reservoir (CHUR) parameters ($^{143}Nd/^{144}Nd$ = 0.512638, $^{147}Sm/^{144}Nd$ = 0.1967) (Jacobsen and Wasserburg, 1984). The model ages T_{Nd}(DM) were calculated from the data for the depleted-mantle reservoir $((^{143}Nd/^{144}Nd)_0$ = 0.513151, $^{147}Sm/^{144}Nd$ = 0.21365) (Goldstein and Jacobsen, 1988). On the calculation of the model ages by the two-stage model (Liew and Hofmann, 1988), the average crustal value of $^{147}Sm/^{144}Nd$ was taken equal to 0.12 (Taylor and McLennan, 1985).

Rb–Sr isotope studies were performed on an MI-1201 T mass spectrometer at the Analytical Center for Multi-Ele-

[1] Xenogenic zircon is zircon borrowed by granite melt from the host rocks. It is older than magmatic zircon and is usually well-faceted. It lacks signs of dissolution of crystal edges and faces and can have rims of newly formed (magmatic) zircon formed at the stage of crystallization of the granite melt. The presence of such zircons does not affect the isotope composition of the granite melt. Inherited zircon is zircon from the source of the granite melt. Such zircons are also older than magmatic ones and have an oval core, which is probably due to their partial dissolution in the granite melt, and a rim of magmatic zircon marking crystallization of the granite melt. Sometimes, there are thin light rims between the cores and magmatic rims, which suggest interaction of the melt with the inherited zircon. The light rims and magmatic rims can have an intermediate isotope composition. Inherited zircons not only mark the age and isotope (Lu–Hf) composition of magma-generating sources (substrates) but also affect the isotope compositions of the melt and magmatic zircon.

Fig. 1. Schematic geologic structure of the Lake Zone, after Tomurtogoo (1999), simplified. *1*, sedimentary deposits (Cenozoic–Mesozoic); *2*, volcanic and sedimentary deposits (Silurian–Devonian); *3*, volcanic and sedimentary deposits (late Neoproterozoic–early Cambrian); *4*, granitoids (Devonian); *5*, granitoids (late Neoproterozoic–Ordovician); *6*, gabbroids (late Neoproterozoic–Early Ordovician); *7*, ophiolites (Neoproterozoic); *8*, faults; *9*, plutons and their numbers: 1, Sharatologoy; 2, Hyargas Nuur; 3, Ayrig Nuur; 4, Bayan Hayrhan; 5, West Bayan Hayrhan; 6, Har Nuur; 7, Gundguzin; 8, Bumbat Hayrhan; 9, Hayrhan; 10, Three Hills; 11, Bayan Tsagaan; 12, East Bayan Tsagaan; 13, Tavan Hayrhan; 14–15, Bayan Tsagaan Nuruu stock; 16, Dut Uul; 17, Bayasgalant; 18, Mandalt; 19, Hatan-Hunga; 20, Tuguruk; 21, Tugrug; 22, Udzur-Hunga; 23, Tungalag; 24, granitoid plutons of the Dariv Range; 25, ophiolites of the Dariv Range; 26, Hara Chulu; 27, Hutul; 28, Sar Hayrhan; *10*, areas of intrusive magmatism: I, Hyargas Nuur; II, Har Nuur; III, Bumbat Hayrhan; IV, Dut Uul; V, Hatan-Hunga; VI, Tugrug; VII, South Darvi; VIII, Haan Tayshiri. Inset shows a schematic tectonic map of Western Mongolia. Precambrian microcontinents: DZ, Dzavhan; SG, South Gobi; LZ, Lake Zone island arc (late Neoproterozoic–early Paleozoic); accretionary complexes (early–middle Paleozoic): MA, Mongolian Altay; SM, South Mongolian.

mental and Isotope Research, SB RAS, Novosibirsk. The error of $^{87}Rb/^{86}Sr$ determination was <1%. The average $^{87}Rb/^{86}Sr$ ratio in the VNIIM and ISG-1 standards was 0.70800 ± 0.00007 (N = 30) and 0.71732 ± 0.00010 (N = 30), respectively.

The isotope composition of Hf in zircons was determined with a Photon Machines Eximer 193 nm laser sampler on a Nu Plasma multicollector mass spectrometer at the GEMOC Analytical Center of Macquarie University (Sydney, Australia). The measurements were carried out in the helium atmosphere, with a laser beam 40–65 μm in diameter, a frequency of 5 Hz, and the laser fluence of 8.44 mJ/pulse. The correction procedure and used values are described elsewhere (Griffin et al., 2004; Pearson et al., 2008). To control the reproducibility of the results and the stability of the device, we used the TEMORA-II and Mud Tank standard zircon samples. The ε_{Hf} values were calculated based on the ^{176}Lu decay constant (Scherer et al., 2001). The model age T(DM) (relative to the evolution trend of the depleted mantle) was estimated from the following isotope ratios: $(^{176}Hf/^{177}Hf)_i$ = 0.279718 (for 4.56 Ga) and $^{176}Lu/^{177}Hf$ = 0.0384. The current $^{176}Hf/^{177}Hf$ ratio was 0.28325, which is close to the average value in MORB (Griffin et al., 2000, 2004). The model ages T(DM) are the minimum ages of the source of magma from which zircon crystallized. Therefore, the model age $T(DM)^{crust}$ was also calculated for each zircon under assumption that magma melted from the average continental crust with the isotope ratio $^{176}Lu/^{177}Hf$ = 0.015, which, in turn, also melted from the depleted mantle (Griffin et al., 2000).

PETROCHEMISTRY AND GEOCHEMISTRY OF GRANITOIDS

Petrochemical and geochemical description of plagiogranitoid associations of the Tugrug, Udzur-Hunga, Hatan-Hunga, Mandalt, Bayasgalant, and Dut Uul plutons in the south of the Lake Zone was made on the basis of more than 90 wet chemical analyses and 35 trace-element and REE analyses. Table 1 presents results of analyses of the studied rocks.

In petrochemical characteristics the plagiogranitoid associations correspond to normal calc-alkalic granitoids with low to medium contents of K_2O and Shand's index of 0.80–1.27 (Rudnev et al., 2019). According to the trace-element composition, they are subdivided into different geochemical types.

Plagiogranitoids of the island-arc stage. At this geodynamic stage of the evolution of the Lake Zone, the rocks of the Tugrug, Udzur-Hunga, Hatan-Hunga, and Bayasgalant plutons formed. The plagiogranitoid associations of these plutons differ significantly from each other in the contents of trace elements and thus can be divided into two types. The first type includes the rocks of diorite–tonalite–plagiogranite association of the Tugrug and Udzur-Hunga plutons and plagiogranite associations of the Hatan-Hunga pluton. They are characterized by medium contents of Rb, Sr, Ba, Nb, Ta, Th, and U (Table 1, Fig. 2), low total contents of REE (15.1–63.5 ppm), domination of LREE over HREE ($(La/Yb)_N$ = 3–11 to 35), high Sr/Y ratios (>70), low contents of Y (1.6–12.2 ppm), positive and negative Eu anomalies (Eu/Eu^*_N = 0.8–1.7), and negative Nb, Ta, and Ti and positive Sr anomalies (Fig. 3). The contents of REE and trace elements, their indicator ratios, and the arrangement of composition points in the Al_2O_3–Yb diagram (Fig. 2) show the similarity of the above rocks to high-alumina tonalite–trondhjemite–granodiorite (TTG) complexes (Arth, 1983). In the binary SiO_2–MgO, (CaO + Na_2O)–Sr, Y–Sr/Y, and TiO_2–Cr/Ni diagrams (Martin et al., 2005; Castillo, 2006), the rocks of the studied associations fall in the field of high-silica adakites. In the Lake Zone, plagiogranitoids with such geochemical characteristics are also found in the West Bayan Hayrhan (Yarmolyuk et al., 2011), Bumbat Hayrhan, and Har Nuur (Rudnev et al., 2009, 2012, 2016) plutons (Fig. 2).

The second type includes the island-arc plagiogranitoid associations of the Bayasgalant pluton (tonalite–plagiogranite and plagiogranite, 524–523 Ma (Rudnev et al., 2019)). Compared with the rock association of the first type, they have lower contents of Al_2O_3 and Sr and higher contents of Y, Yb, Nb, Hf, and Zr and form isolated fields in the binary diagrams (Table 1, Fig. 2). These rocks show medium contents of REE (ΣREE = 48–66 ppm), low $(La/Yb)_N$ values (1.7–3.1) (mostly because of the high contents of HREE (Fig. 3)), low Sr/Y ratios (5–11), negative Nb, Ta, and Ti anomalies, and no positive Sr anomaly. In the contents of Al_2O_3, trace elements, and REE, their indicator ratios, and the arrangement of composition points in the Al_2O_3–Yb diagram (Fig. 2) the rocks of the Bayasgalant pluton are similar to low-alumina plagiogranitoids. In the Lake Zone, plagiogranitoid associations of close age and similar composition are found within the Sharatologoy and Har Nuur plutons and the Darvi intrusion (Rudnev et al., 2009, 2016).

Plagiogranitoid associations of the accretion–collision stage. At this geodynamic stage of evolution of the southern part of the Lake Zone, plagiogranitoids of the Tugrug, Dut Uul, and Mandalt plutons formed. In petrochemical composition, the contents of trace and rare-earth elements, and indicator ratios the muscovite–biotite and biotite plagiogranites of the Tugrug (late phase, ~504 Ma) and Dut Uul (~481 Ma) plutons virtually do not differ from the plagiogranitoids of the Hatan-Hunga pluton of the island-arc stage and are also of high-alumina type (Fig. 2). In the binary SiO_2–MgO, (CaO + Na_2O)–Sr, Y–Sr/Y, and TiO_2–Cr/Ni diagrams, their composition points fall in the field of high-silica adakites. In the Lake Zone, high-alumina plagiogranites of similar trace-element composition (Fig. 3) are also found in the Bumbat Hayrhan and Har Nuur plutons (Fig. 1) (Rudnev et al., 2009, 2012, 2016).

In contrast to all the above plagiogranitoid associations in the south of the Lake Zone, the quartz diorites and tonalites

Table 1. Contents of major and trace components in representative samples of plagiogranitoid plutons in the south of the Lake Zone of Western Mongolia

Component	Tugrug pluton Diorite–tonalite–plagiogranite association (early phase)								Tugrug pluton Plagiogranite association (late phase)			
	PM-31-11	PM-37-11	PM-37-11	PM-37-11	PM-37-11	PM-19-13	PM-20-13	PM-7-13	PM-37-11	PM-24-13	PM-40-11	PM-38-11
SiO_2, wt.%	57.77	60.45	62.31	63.25	63.81	64.28	67.82	71.15	71.21	71.56	71.88	72.58
TiO_2	0.45	0.44	0.40	0.44	0.43	0.43	0.20	0.27	0.03	0.02	0.03	0.03
Al_2O_3	19.10	19.20	18.35	18.70	17.80	17.22	17.80	15.04	16.70	15.33	16.05	15.95
$Fe_2O_{3\ tot}$	6.28	5.39	4.93	4.22	4.40	4.71	2.40	2.63	2.34	2.55	1.75	2.15
MnO	0.10	0.08	0.08	0.07	0.09	0.09	0.03	0.07	0.06	0.06	0.03	0.06
MgO	2.86	2.14	1.74	1.49	2.02	1.75	0.62	0.86	0.45	0.49	0.49	0.45
CaO	6.53	5.65	5.13	5.04	5.20	5.06	4.53	2.66	1.70	2.37	1.74	1.30
Na_2O	4.71	4.77	4.98	5.28	4.43	4.65	5.04	4.54	5.47	5.19	5.99	5.37
K_2O	1.15	1.05	1.05	0.74	1.42	1.26	1.06	1.87	1.42	1.28	0.73	1.36
LOI	1.21	0.89	0.69	0.82	0.86	0.57	0.95	0.53	0.75	0.60	0.95	0.81
P_2O_5	0.21	0.21	0.20	0.17	0.14	0.19	0.12	0.09	0.05	0.05	0.03	0.04
Total	100.37	100.27	99.86	100.22	100.60	100.20	100.58	99.70	100.18	99.50	99.67	100.10
Rb, ppm	15	14	13	12	19	13	9	25	14	9	8	15
Sr	890	912	895	949	823	791	823	587	690	668	901	652
Ba	389	396	415	348	388	441	372	512	696	583	321	570
Y	12.22	11.37	11.03	7.68	10.50	9.19	3.59	7.02	4.22	4.55	5.50	8.64
Zr	65	114	108	88	79	97	73	64	73	56	66	64
Hf	1.65	2.58	2.62	1.96	2.09	2.70	2.01	1.97	1.75	1.58	1.60	1.53
Nb	1.91	1.87	1.99	1.40	1.99	1.97	1.01	3.33	1.59	1.45	1.72	1.66
Ta	0.09	0.10	0.11	0.08	0.13	0.11	0.09	0.29	0.11	0.11	0.11	0.11
Th	0.86	1.29	1.09	0.53	2.37	1.81	1.42	2.19	0.46	0.48	0.53	0.40
U	0.30	0.40	0.46	0.23	0.72	0.73	0.60	0.65	0.17	0.14	0.13	0.23
V	122	102	87	83	87	97	41	32	19	20	17	16
Cr	30	36	22	54	29	31	50	27	46	22	23	38
Co	19	16	13	11	13	11	5	5	3	2	3	3
Ni	23	16	14	18	15	11	6	7	11	3	11	12
La	9.82	11.71	10.20	6.65	8.95	11.44	6.89	7.88	7.06	5.90	6.49	5.74
Ce	21.74	24.78	23.90	15.38	19.81	26.10	13.97	19.18	14.55	12.07	13.47	11.82
Pr	3.00	3.28	3.32	2.16	2.67	3.32	1.65	2.54	1.81	1.39	1.59	1.40
Nd	11.98	13.13	13.64	8.93	10.95	12.84	6.34	9.25	6.40	4.96	5.78	5.23
Sm	2.44	2.84	2.81	1.95	2.37	2.56	1.14	1.89	1.16	0.95	1.05	1.06
Eu	0.76	0.83	0.86	0.69	0.72	0.83	0.52	0.47	0.28	0.29	0.28	0.29
Gd	2.30	2.32	2.28	1.56	1.99	2.20	0.89	1.53	0.92	0.81	0.86	1.19
Tb	0.33	0.30	0.33	0.24	0.30	0.29	0.13	0.19	0.12	0.12	0.14	0.18
Dy	1.92	1.80	1.75	1.17	1.65	1.52	0.59	1.08	0.63	0.67	0.71	1.08
Ho	0.39	0.36	0.33	0.24	0.30	0.32	0.12	0.22	0.12	0.13	0.15	0.23
Er	1.08	0.93	0.95	0.72	0.90	0.88	0.37	0.62	0.33	0.43	0.45	0.66
Tm	0.16	0.14	0.14	0.10	0.15	0.14	0.06	0.11	0.06	0.08	0.08	0.11
Yb	0.96	0.90	0.87	0.63	0.96	0.99	0.40	0.72	0.36	0.50	0.56	0.69
Lu	0.15	0.13	0.13	0.10	0.15	0.15	0.07	0.11	0.06	0.08	0.09	0.11
ΣREE	57.04	63.46	61.51	40.53	51.88	62.58	33.14	45.79	33.86	28.38	31.69	29.80
$(La/Yb)_N$	6.9	8.8	7.9	7.1	6.3	7.8	11.6	7.4	13.1	8.0	7.8	5.6
$(Eu/Eu^*)_N$	1.0	1.0	1.0	1.2	1.0	1.0	1.5	0.8	0.8	1.0	0.9	0.8
Sr/Y	73	80	81	124	78	86	229	84	164	147	164	75

Table 1 (*continued*)

Component	Udzur-Hunga pluton Diorite–tonalite–plagiogranite association				Hatan-Hunga pluton Plagiogranite association			Mandalt pluton Diorite–tonalite–plagiogranite association			
	PM-18-11	PM-16-11	PM-19-15	PM-19/1-11	PM-37-13	PM-36-13	PM-34-13	PM-26-14	PM-25-14	PM-21-14	PM-23-14
SiO_2, wt.%	57.53	60.21	62.58	74.88	71.82	72.40	73.70	58.05	59.29	64.68	67.20
TiO_2	0.50	0.55	0.42	0.08	0.13	0.10	0.10	0.66	0.57	0.31	0.41
Al_2O_3	19.25	18.60	17.27	14.20	15.87	15.47	15.32	17.42	17.13	17.40	16.14
$Fe_2O_{3\,tot}$	6.47	6.00	5.62	2.14	1.93	1.89	1.69	5.81	5.57	4.41	2.92
MnO	0.13	0.10	0.10	0.02	0.07	0.06	0.07	0.08	0.08	0.05	0.03
MgO	3.28	2.64	2.27	0.23	0.37	0.31	0.37	3.48	3.80	1.46	1.60
CaO	7.10	6.31	5.43	3.09	2.42	2.19	1.81	5.94	5.72	3.66	3.87
Na_2O	4.16	4.32	4.17	4.21	5.37	5.51	5.59	4.72	4.72	5.02	4.69
K_2O	0.83	0.90	0.89	0.37	1.22	0.96	1.03	1.28	0.97	1.49	0.86
LOI	1.25	0.80	1.07	0.41	0.92	0.59	0.87	2.15	1.27	1.04	1.50
P_2O_5	0.16	0.16	0.13	0.02	0.06	0.07	0.05	0.22	0.20	0.11	0.13
Total	100.66	100.59	99.96	99.65	100.16	99.55	100.61	99.81	99.30	99.63	99.34
Rb, ppm	9	10	9	4	14	10	11	28	22	32	22
Sr	809	781	720	597	592	540	521	805	781	727	739
Ba	363	373	500	285	746	649	883	440	335	468	360
Y	10.50	9.05	8.26	1.59	2.91	5.37	4.12	13.42	11.08	2.86	2.91
Zr	29	60	56	43	59	51	51	111	68	75	106
Hf	0.87	1.39	1.53	1.28	1.64	1.49	1.48	2.76	1.92	2.01	2.33
Nb	0.83	0.92	0.96	0.29	1.45	1.12	1.01	3.44	2.79	2.43	2.85
Ta	0.05	0.06	0.05	0.04	0.08	0.06	0.06	0.24	0.21	0.27	0.18
Th	0.46	0.26	0.63	1.96	0.39	0.23	0.14	3.11	2.80	2.83	4.85
U	0.26	0.23	0.21	0.30	0.11	0.11	0.09	1.11	0.60	0.84	0.60
V	162	143	115	21	13	8	7	109	93	50	45
Cr	42	48	37	95	44	60	24	110	126	135	51
Co	22	19	13	4	2	2	2	16	16	8	10
Ni	22	18	15	30	11	8	9	56	69	30	41
La	4.74	4.35	4.77	7.50	3.29	2.52	2.43	15.52	12.40	9.10	11.62
Ce	10.62	9.97	10.63	14.92	7.03	5.75	5.54	33.10	27.18	16.23	18.53
Pr	1.51	1.49	1.55	1.40	0.85	0.78	0.73	3.85	3.20	1.50	1.50
Nd	6.99	6.36	6.11	4.60	3.60	3.41	3.00	15.80	13.30	5.40	4.90
Sm	1.75	1.53	1.22	0.60	0.68	0.69	0.66	3.52	2.84	0.95	0.86
Eu	0.73	0.62	0.52	0.29	0.19	0.16	0.20	1.09	1.03	0.58	0.45
Gd	1.81	1.57	1.45	0.41	0.56	0.71	0.64	2.89	2.57	0.74	0.56
Tb	0.30	0.24	0.23	0.05	0.08	0.12	0.10	0.46	0.35	0.10	0.08
Dy	1.65	1.36	1.36	0.18	0.43	0.75	0.58	2.37	1.96	0.46	0.38
Ho	0.33	0.27	0.28	0.04	0.09	0.18	0.13	0.48	0.40	0.09	0.08
Er	0.90	0.77	0.85	0.12	0.29	0.54	0.40	1.24	1.05	0.27	0.23
Tm	0.14	0.12	0.13	0.03	0.05	0.08	0.08	0.19	0.16	0.04	0.03
Yb	0.93	0.71	0.89	0.18	0.36	0.55	0.53	1.13	0.99	0.27	0.22
Lu	0.14	0.11	0.13	0.03	0.06	0.08	0.08	0.17	0.15	0.04	0.03
ΣREE	32.54	29.47	30.11	30.38	17.56	16.32	15.11	81.80	67.58	35.78	39.46
$(La/Yb)_N$	3.4	4.1	3.6	28	6.2	3.1	3.1	9.3	8.4	22.8	35.6
$(Eu/Eu^*)_N$	1.2	1.2	1.2	1.7	0.9	0.7	0.9	1.0	1.1	2.0	1.9
Sr/Y	77	86	87	375	203	101	126	60	71	255	254

Table 1 (*continued*)

Component	Bayasgalant pluton								Dut Uul pluton				
	Tonalite–plagiogranite association (early phase)					Plagiogranite association (late phase)			Plagiogranite association				
	PM-38-14	PM-35-14	PM-30/2-14	PM-30-14	PM-31-14	PM-28-14	PM-29-14	PM-33-14	PM-10-11	PM-13-11	PM-4-11	PM-63-08	PM-62-08
SiO_2, wt.%	66.31	67.95	70.14	72.17	73.05	71.50	72.33	72.54	68.60	71.36	71.78	71.27	71.27
TiO_2	0.47	0.44	0.34	0.33	0.31	0.30	0.29	0.23	0.21	0.18	0.16	0.03	0.15
Al_2O_3	15.06	14.80	14.29	13.43	13.57	13.76	13.78	13.50	18.10	16.25	16.20	15.45	15.70
$Fe_2O_{3\ tot}$	5.30	4.94	3.93	3.99	3.35	3.45	3.39	2.97	2.24	2.29	1.77	2.35	2.19
MnO	0.11	0.11	0.09	0.09	0.09	0.07	0.07	0.08	0.03	0.05	0.03	0.05	0.05
MgO	1.58	1.56	1.17	0.79	0.75	0.84	0.76	0.64	0.52	0.38	0.34	0.50	0.50
CaO	4.01	3.89	3.01	2.64	2.42	2.52	2.39	2.60	3.73	1.94	3.00	3.75	3.56
Na_2O	4.11	3.85	4.40	4.16	4.24	4.15	4.07	4.29	5.33	5.15	5.02	5.03	5.34
K_2O	1.04	1.20	1.35	1.60	1.64	1.76	1.81	1.44	0.62	1.33	1.11	0.49	0.48
LOI	1.02	0.81	1.32	0.72	0.78	0.66	0.75	0.76	0.77	1.25	0.75	0.88	0.70
P_2O_5	0.09	0.09	0.07	0.06	0.06	0.06	0.06	0.05	0.06	0.05	0.07	0.04	0.03
Total	99.11	99.64	100.09	99.98	100.27	99.09	99.71	99.09	100.21	100.23	100.23	99.84	99.97
Rb, ppm	15	22	24	28	23	28	30	25	7	20	15	9	6
Sr	255	224	215	151	174	217	232	235	672	416	481	563	462
Ba	337	372	385	454	482	717	762	613	274	575	487	422	409
Y	22.72	22.18	22.96	28.80	30.78	27.86	27.65	27.88	5.38	6.61	6.27	9.34	5.97
Zr	139	160	144	168	151	141	148	119	92	90	77	99	394
Hf	3.23	3.59	3.55	4.17	3.84	3.36	3.51	3.04	2.07	2.28	1.93	2.26	9.26
Nb	3.10	2.93	3.01	3.26	3.31	3.83	3.41	2.94	1.15	1.52	1.52	1.19	1.46
Ta	0.21	0.21	0.24	0.24	0.24	0.24	0.18	0.24	0.07	0.11	0.09	0.08	0.11
Th	1.82	2.12	2.60	2.62	2.66	2.69	2.85	2.13	0.36	0.48	1.03	0.66	0.63
U	0.63	0.69	1.05	0.95	1.11	0.99	1.02	1.15	0.18	0.21	0.21	0.21	0.83
V	62	64	41	26	26	24	23	21	17	13	13	13	10
Cr	47	30	43	88	41	44	55	56	7	57	8	15	16
Co	10	10	7	5	5	5	5	4	3	3	2	3	
Ni	18	12	11	11	8	8	13	15	21	30	18	21	
La	7.47	8.41	10.04	10.42	10.22	10.18	9.05	6.29	2.91	3.41	4.98	3.95	3.49
Ce	17.31	19.03	21.76	24.10	23.40	23.19	20.61	14.747	5.93	7.28	9.80	8.72	7.64
Pr	2.05	2.20	2.50	2.88	2.86	2.88	2.46	1.92	0.75	0.91	1.22	1.17	0.88
Nd	8.80	9.20	9.90	12.08	12.07	12.33	10.54	8.77	3.03	3.68	4.97	4.36	3.92
Sm	2.50	2.42	2.42	3.15	3.29	3.25	2.73	2.45	0.63	0.88	0.85	1.05	0.85
Eu	0.84	0.79	0.72	0.80	0.78	0.61	0.53	0.61	0.21	0.15	0.19	0.30	0.24
Gd	2.40	2.38	2.22	2.80	2.89	2.92	2.51	2.47	0.59	0.80	0.75	0.89	0.63
Tb	0.42	0.42	0.42	0.55	0.58	0.56	0.54	0.53	0.09	0.11	0.13	0.15	0.11
Dy	2.91	2.79	2.89	3.71	3.90	3.57	3.56	3.59	0.57	0.71	0.73	0.84	0.75
Ho	0.64	0.64	0.63	0.80	0.87	0.73	0.78	0.78	0.14	0.16	0.15	0.16	0.16
Er	1.93	1.92	1.97	2.47	2.68	2.25	2.38	2.40	0.41	0.49	0.44	0.50	0.48
Tm	0.32	0.31	0.33	0.42	0.43	0.38	0.38	0.38	0.06	0.08	0.08	0.08	0.09
Yb	2.07	2.07	2.20	2.80	2.97	2.68	2.51	2.50	0.43	0.52	0.52	0.50	0.70
Lu	0.32	0.32	0.35	0.43	0.44	0.41	0.38	0.39	0.06	0.08	0.08	0.08	0.15
ΣREE	49.98	52.88	58.35	67.41	67.37	65.96	58.96	47.82	15.81	19.26	24.88	22.75	20.10
$(La/Yb)_N$	2.4	2.7	3.1	2.5	2.3	2.6	2.4	1.7	4.6	4.5	6.5	5.3	3.4
$(Eu/Eu^*)_N$	1.0	1.0	0.9	0.8	0.8	0.6	0.6	0.8	1.1	0.6	0.7	0.9	1.0
Sr/Y	11	10	9	5	6	8	8	8	129	63	77	60	116

Note. The contents of major components were determined by XRF at the Analytical Center for Multi-Elemental and Isotope Research, SB RAS, Novosibirsk, using an SRM-25 spectrometer (analysts N.G. Karmanova and A.N. Toryanik). The contents of trace and rare-earth elements were measured by ICP MS on a Finnigan Element mass spectrometer at the same analytical center, following the technique by Nikolaeva et al. (2008); the errors of their determination were <10%.

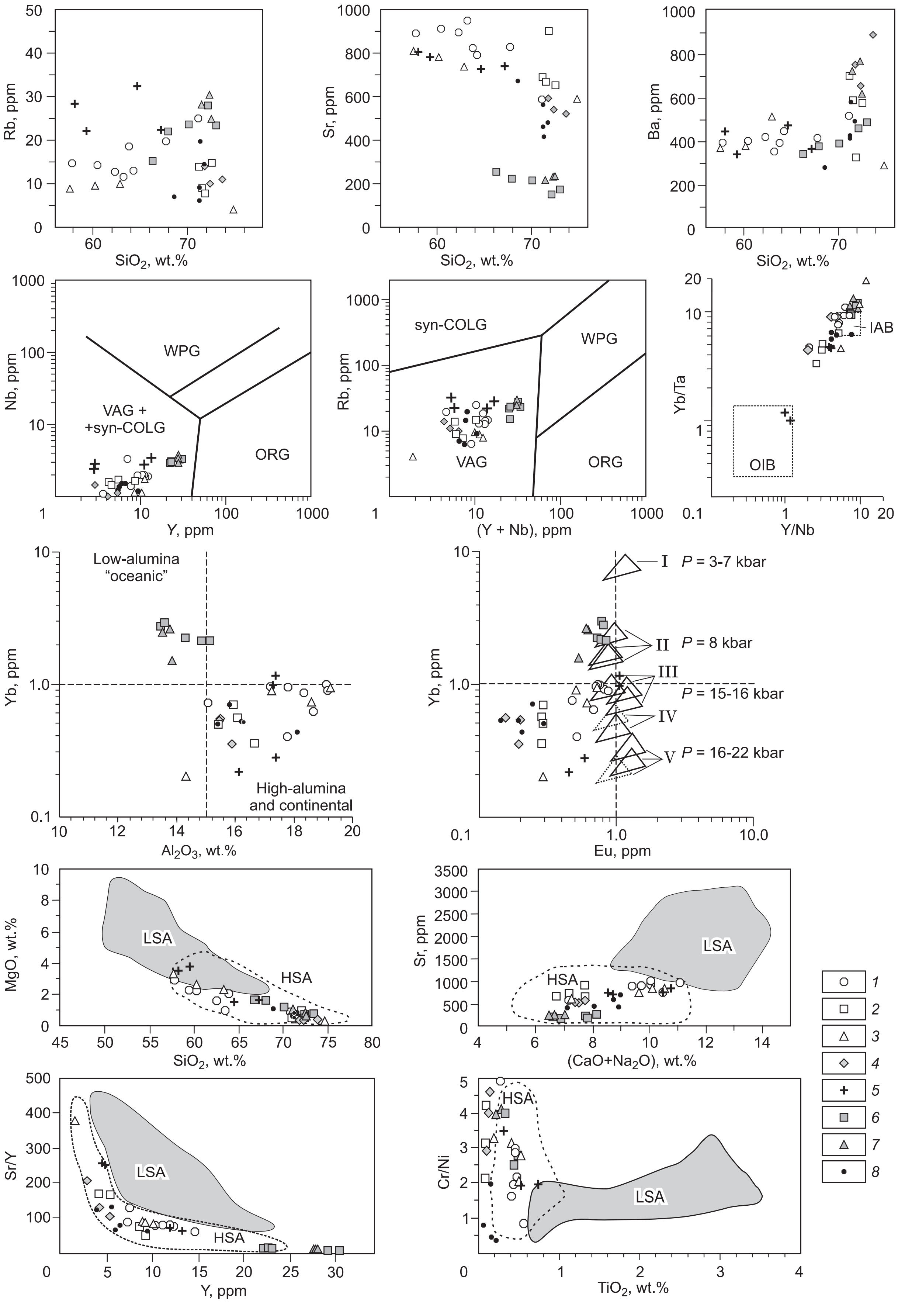
Rb, ppm
SiO2, wt.%
Sr, ppm
SiO2, wt.%
Ba, ppm
SiO2, wt.%
Nb, ppm
WPG
VAG +
+syn-COLG
ORG
Y, ppm
Rb, ppm
syn-COLG
WPG
VAG
ORG
(Y + Nb), ppm
Yb/Ta
IAB
OIB
Y/Nb
Low-alumina
"oceanic"
High-alumina
and continental
Yb, ppm
Al2O3, wt.%
I P = 3-7 kbar
II P = 8 kbar
III
P = 15-16 kbar
IV
V P = 16-22 kbar
Yb, ppm
Eu, ppm
MgO, wt.%
LSA
HSA
SiO2, wt.%
Sr, ppm
HSA
LSA
(CaO+Na2O), wt.%
Sr/Y
LSA
HSA
Y, ppm
Cr/Ni
HSA
LSA
TiO2, wt.%
1
2
3
4
5
6
7
8

Fig. 2. Discrimination diagrams for the early Paleozoic granitoids in the south of the Lake Zone. *1*, *2*, Tugrug pluton (*1*, diorite–tonalite–plagiogranite association, early phase, 531 Ma; *2*, plagiogranite association, late phase, 504 Ma); *3*, Udzur-Hunga pluton (diorite–tonalite–plagiogranite association, 517 Ma); *4*, Hatan-Hunga pluton (plagiogranite association, 521 Ma); *5*, Mandalt pluton (diorite–tonalite–plagiogranite association, 495 Ma); *6*, *7*, Bayasgalant pluton (*6*, tonalite–plagiogranite association, early phase, 524 Ma, *7*, plagiogranite association, late phase, 522 Ma); *8*, Dut Uul pluton (plagiogranite association, 481 Ma). The results of rock analyses are listed in Table 1. Diagrams: SiO_2–Rb, SiO_2–Sr, SiO_2–Ba, Y–Nb, and (Y + Nb)–Rb (Pearce et al., 1984), WPG, within-plate granites, ORG, oceanic-ridge granites, syn-COLG, syncollisional granites, VAG, volcanic-arc granites; Y/Nb–Yb/Ta (Eby, 1990), IAB, island-arc basalts; OIB, oceanic-island basalts; Al_2O_3–Yb (Arth, 1979); Eu–Yb (Turkina, 2000); SiO_2–MgO, Sr–(CaO + Na_2O), Sr/Y–Y, and Cr/Ni–TiO_2 (Martin et al., 2005; Castillo, 2006). The diagrams show that the studied early Paleozoic plagiogranitoid associations are high- and low-alumina TTG complexes. Triangles in the Eu–Yb diagram mark the domains of the element contents in melts produced under dehydration (solid lines) and aqueous (dotted lines) melting of the sources of TH1, TH2, and MORB (Rapp et al., 1991; Beard and Lofgren, 1991; Rapp and Watson, 1995) in equilibrium with five types of restites (Turkina, 2000): I, Pl + Cpx + Opx, II, Hbl + Pl ± Cpx ± Opx, III, IV, Hbl + Cpx + Pl ± Grt, and V, Cpx + Grt ± Hbl. Pl, plagioclase; Cpx, clinopyroxene; Opx, orthopyroxene; Hbl, amphibole; Grt, garnet; LSA, low-silica adakites; HSA, high-silica adakites.

of the Mandalt pluton (~495 Ma) show high contents of MgO, P_2O_5, Rb, Nb, Ta, Th, U, Zr, Hf, V, Cr, Co, and Ni (Table 1) and form an isolated composition field in the SiO_2–Rb, Y–Nb, and Y/Nb–Yb/Ta diagrams (Fig. 2). In the contents of trace and rare-earth elements these rocks are also similar to high-alumina TTG complexes.

RESULTS OF ISOTOPE STUDY

Sm–Nd *and* Rb–Sr *isotope characteristics of rocks*

The studied plagiogranitoids have different Sr–Nd isotope characteristics (Table 2, Fig. 4).

The early- and late-phase high-alumina plagiogranitoid associations of the Tugrug, Udzur-Hunga, Hatan-Hunga, and Dut Uul plutons are characterized by high positive values of $\varepsilon_{Nd}(T)$, varying from 8.5 to 6.1, $T_{Nd}(DM)$ = 0.74–0.58 Ga, and low Sr isotope ratios (($^{87}Sr/^{86}Sr)_0$ = 0.7034–0.7037). In the ε_{Nd}–age diagram (Fig. 4), their isotope composition points fall in the field of island-arc complexes (volcanics and granitoids) of the Lake Zone (Kovalenko et al., 2004; Rudnev et al., 2009; Kovach et al., 2011; Kröner et al., 2014).

The low-alumina plagiogranitoid (tonalite–plagiogranite and plagiogranite) associations of the Bayasgalant pluton show lower values of ε_{Nd} (6.8–4.6) than the high-alumina ones. However, the ε_{Nd} values of the two associations partly overlap.

High-alumina plagiogranitoids of the Mandalt pluton differ from all the above plagiogranitoid associations of the southern Lake Zone. They are characterized by low ε_{Nd} values (0.2–1.4), older Nd model ages (T_{Nd}(DM) = 1.23–1.12 Ga), and high strontium isotope ratios (($^{87}Sr/^{86}Sr)_0$ = 0.70527). In Fig. 4, their Nd isotope composition points lie between the field of the island-arc volcanics of the Lake Zone and the early Precambrian rocks of the Dzavhan microcontinent.

Hf *isotope systematization of magmatic zircons*

Analyses of magmatic zircons (Table 3, Figs. 5 and 6) from the island-arc plagiogranitoid associations of the Tugrug (sample PM-26-11), Hatan-Hunga (sample PM-34-13), and Bayasgalant (sample PM-31-14 and PM-28-14) plutons showed narrow ranges of ε_{Hf} values (14.6–11.9) and model ages (T_{DM}^{cryst} = 0.7–0.5 Ga). In the ε_{Hf}–age diagram (Fig. 6) they form a compact composition field near the line of the depleted mantle.

Magmatic zircons from plagiogranitoid associations of the accretion–collision stage of evolution of the Lake Zone have a wider range of Hf isotope parameters and thus can be divided into two groups. The first group includes zircons from the late-phase plagiogranites of the Tugrug (sample PM-34-13) and Dut Uul (sample RM-62-08) plutons, characterized by high positive values of ε_{Hf} (14.2–9.3) and T_{DM}^{cryst} = 0.8–0.5 Ga. In these isotope parameters they virtually do not differ from zircons of island-arc plagiogranitoids. The second group includes magmatic zircons from the plagiogranitoids of the Mandalt pluton, with lower ε_{Hf} values (7.2–5.4) and T_{DM}^{cryst} = 1.0 Ga. As seen from the ε_{Hf}–age diagram (Fig. 6), the studied population of magmatic zircons from this pluton forms an isotope composition field isolated from the fields of zircons from the other plutons.

Hf *isotope systematization of inherited and xenogenic zircons*

The inherited and xenogenic zircons from the regional island-arc and accretion–collision plagiogranitoids have a wide range of ages, from 664 to 519 Ma (Rudnev et al., 2019). The Lu–Hf isotope study of these zircons shows significant variations in their isotope parameters (Table 3, Figs. 5 and 6).

The inherited zircons from the early- and late-phase island-arc plagiogranitoids of the Bayasgalant pluton (539–535 Ma) are characterized by a narrow range of $\varepsilon_{Hf}(T)$ values, 12.8–14.7, and $T(DM)^{crust}$ = 0.7–0.5 Ga. In these isotope parameters they do not differ from the overgrowing magmatic zircons and from the magmatic zircon from the island-arc plagiogranitoids of the Tugrug and Hatan-Hunga plutons (Fig. 6). These zircons form a single composition field near the line of the depleted mantle. The inherited zircons with ages of 664 and 545 Ma from the island-arc plagiogranites of the Hatan-Hunga pluton show lower ε_{Hf} values ($\varepsilon_{Hf}(664)$ = 10.6 and $\varepsilon_{Hf}(545)$ = 6.7) than the overgrowing zircons ($\varepsilon_{Hf}(T)$ = 14.0–12.8).

The inherited zircons from the regional accretion–collision plagiogranitoids show a wider range of $\varepsilon_{Hf}(T)$ values

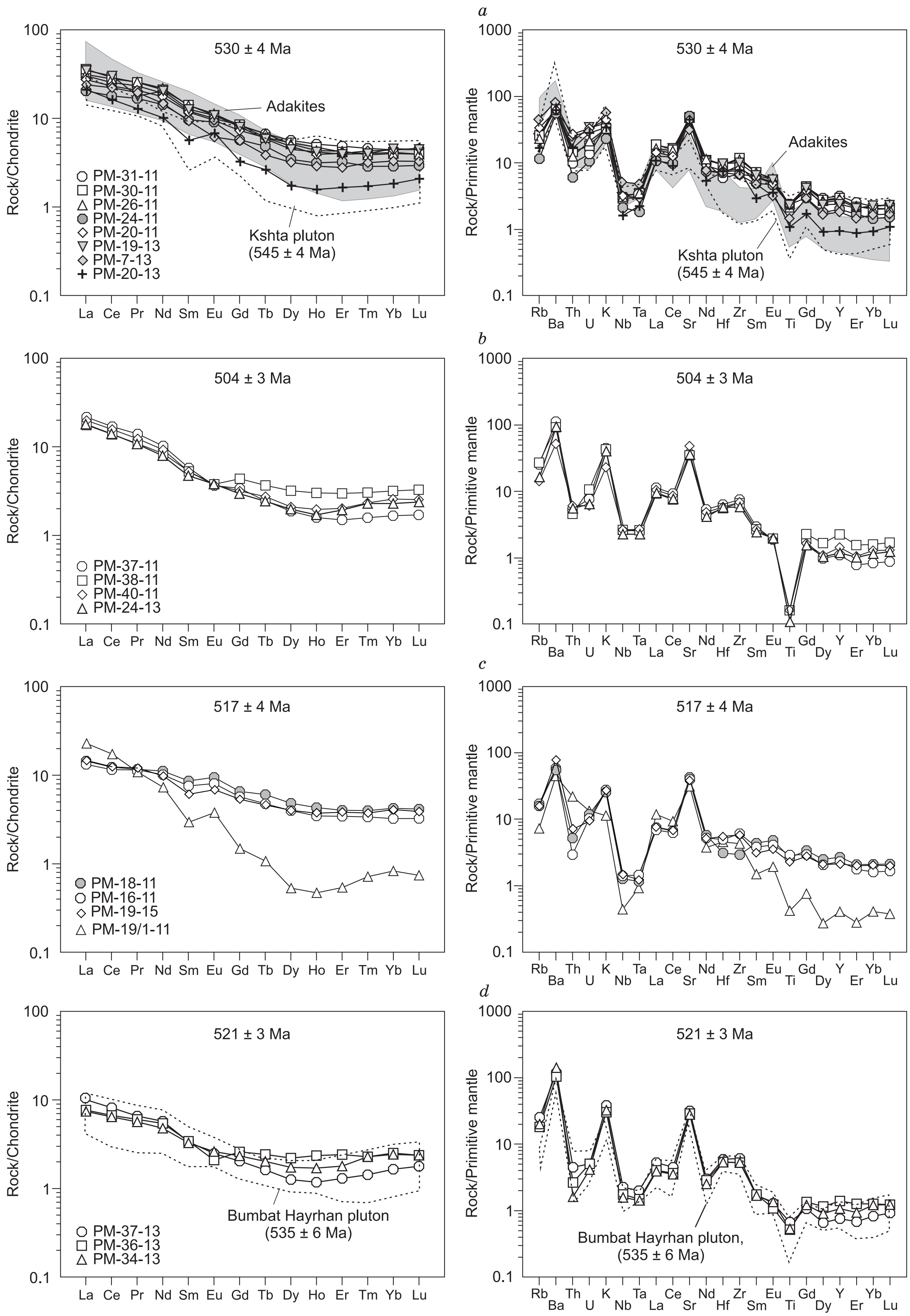

Fig. 3. Chondrite- and primitive-mantle-normalized (Sun and McDonough, 1989) multielement patterns of early Paleozoic plagiogranitoids from the south of the Lake Zone. *a*, *b*, Tugrug pluton: *a*, early phase, *b*, late phase; *c*, Udzur-Hunga pluton; *d*, Hatan-Hunga pluton; *e*, Mandalt pluton; *f*, *g*, Bayas-galant pluton: *f*, early phase, *g*, late phase; *h*, Dut Uul pluton. Gray field marks the composition of adakites, after Martin et al. (2005) and Castillo (2006).

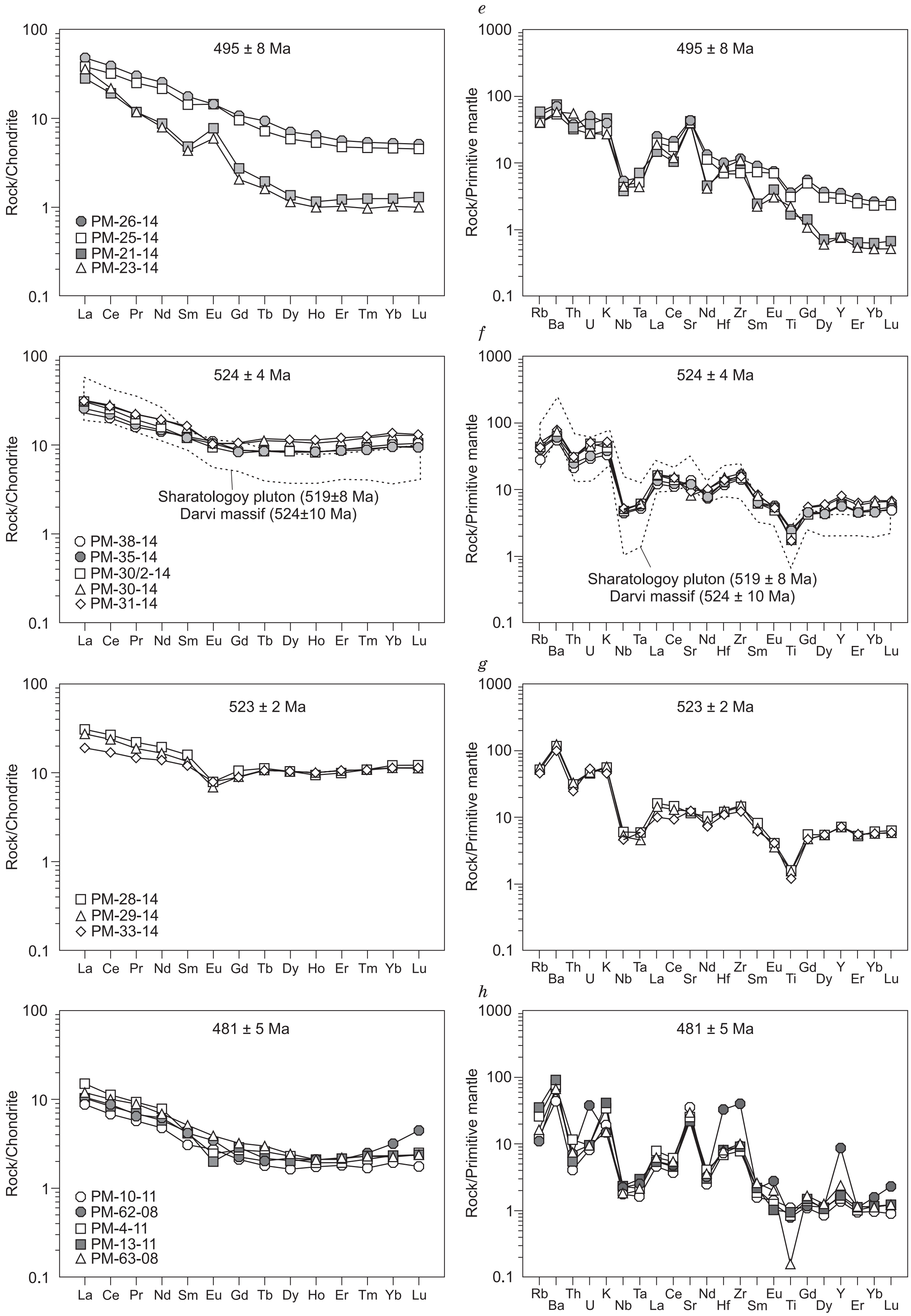

Fig. 3. (*continued*)

and can be divided into two groups according to isotope parameters. The first group includes zircons with an age of 540–524 Ma from the late-phase plagiogranites of the Tugrug and Dut Uul plutons. They are characterized by a narrow range of $\varepsilon_{Hf}(T)$ values, 14.0–13.8 (Table 3, Fig. 6), which does not differ from that of the inherited and magmatic zircons from the island-arc plagiogranitoids of the Bayasgalant, Tugrug, and Hatan-Hanga plutons. The xenogenic zircons with an age of 530–519 Ma can also be included into this group. They are found in the Mandalt pluton and were borrowed from the host rocks during the pluton formation (Rudnev et al., 2019). Nevertheless, they do not differ in isotope parameters ($\varepsilon_{Hf}(T)$ = 13.9–13.5) from the above-described inherited zircons of the same group.

The second group includes inherited zircons with an age of 563 Ma present in late-phase plagiogranites of the Tugrug pluton. In contrast to all the inherited zircons of the first group, they are characterized by low $\varepsilon_{Hf}(T)$ values (2.9) and an older model age ($T(DM)^{crust}$ = 1.3 Ga) (Fig. 6).

DISCUSSION

The trace-element composition of plagiogranitoids and the formation conditions of the parental melts

Study of the petrochemical composition of the early Paleozoic plagiogranitoid associations in the south of the Lake Zone showed that they are calc-alkalic TTG (Rudnev et al., 2019). These rocks are subdivided into low- and high-alumina types.

The island-arc stage of evolution of the southern Lake Zone (531–517 Ma) is marked by the formation of low- and high-alumina plagiogranitoids. The early-phase diorite–tonalite–plagiogranite associations of the Tugrug (531 ± 4 Ma) and Udzur-Honga (517 ± 4 Ma) plutons and the plagiogranite association of the Hatan-Hunga pluton (521 ± 3 Ma) are predominant. In geochemical features, indicator ratios, and trace-element and REE patterns they are similar to high-silica adakites (Figs. 2 and 3). This fact suggests that the parental melts for the studied associations were generated from N-MORB in equilibrium with the Hbr + CPx + Pl ± Gar restite at ≥10–12 kbar during the subduction of the oceanic plate.

Within the southern Lake Zone, island-arc low-alumina plagiogranitoid associations are found only in the Bayasgalant pluton. Taking into account the age (524–522 Ma) and geodynamic setting of formation of its rocks and their trace-element composition, we assume that the rocks formed through the partial melting of MORB-type metavolcanics in equilibrium with the Hbr + Pl ± CPx ± OPx restite in the basement of an island-arc system at ≤8 kbar (Fig. 2).

The accretion-collision stage of evolution of the southern Lake Zone (504–481 Ma) was characterized by the formation of only high-alumina plagiogranitoids. These are rocks of the Tugrug (504 ± 3 Ma), Dut Uul (481 ± 3 Ma), and Mandalt (495 ± 8 Ma) plutons. Judging from their trace-element composition and indicator ratios and the arrange-

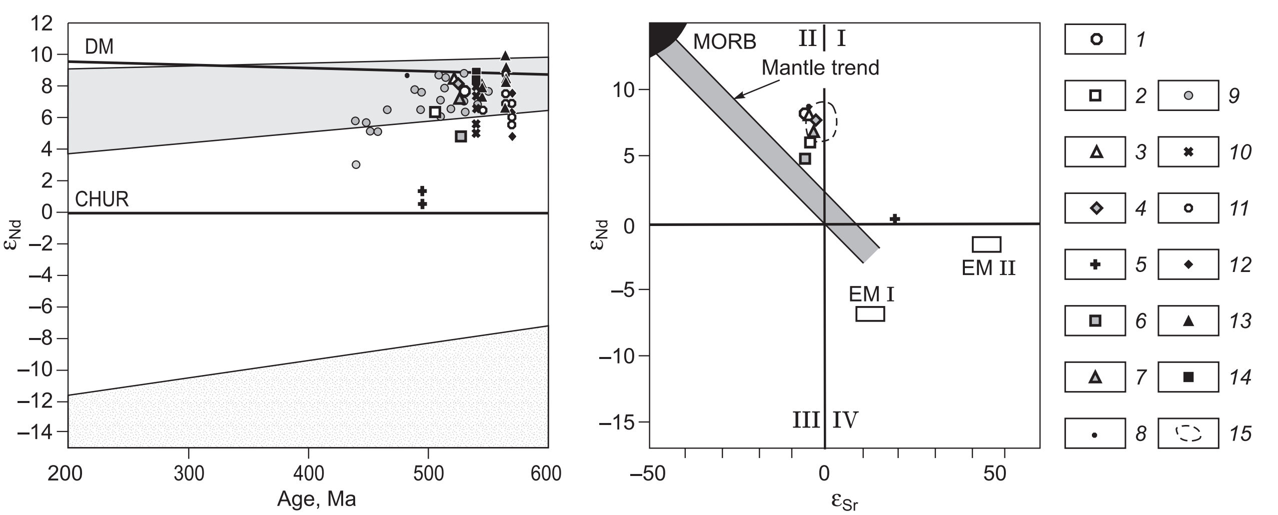

Fig. 4. ε_{Nd}–age and ε_{Nd}–ε_{Sr} diagrams for early Paleozoic plagiogranitoid associations of the Lake Zone. *1–8*, isotope parameters of plagiogranitoids in the south of the Lake Zone (Table 2): *1*, *2*, Tugrug pluton (*1*, diorite–tonalite–plagiogranite association, early phase, 531 Ma; *2*, plagiogranite association, late phase, 504 Ma); *3*, Udzur-Hunga pluton (diorite–tonalite–plagiogranite association, 517 Ma); *4*, Hatan-Hunga pluton (plagiogranite association, 521 Ma); *5*, Mandalt pluton (diorite–tonalite–plagiogranite association, 495 Ma); *6*, *7*, Bayasgalant pluton (*6*, tonalite–plagiogranite association, early phase, 524 Ma, *7*, plagiogranite association, late phase, 522 Ma); *8*, Dut Uul pluton (plagiogranite association, 481 Ma); *9*, Paleozoic granitoid associations of the Lake Zone (Kovalenko et al., 2004; Rudnev et al., 2009, 2013; Kovach et al., 2011); *10–14*, isotope parameters (Kovach et al., 2011; Kröner et al., 2014): *10*, sedimentary rocks of accretionary prisms; *11*, sedimentary deposits in association with volcanics; *12*, oceanic-plateau volcanics; *13,* island-arc volcanics; *14*, back-arc basin volcanics; *15*, plagiogranitoid associations in the northern and central parts of the Lake Zone (Rudnev et al., 2009, 2013). In the ε_{Nd}–age diagram, the gray and speckled fields mark the evolution of the Nd isotope composition of island-arc volcanics of the Lake Zone and Precambrian rocks of the Dzavhan microcontinent, respectively (Kovach et al., 2011; Kröner et al., 2014).

Table 2. Results of Sm–Nd and Rb–Sr isotope studies of early Paleozoic plagiogranitoid associations in the south of the Lake Zone

No.	Sample	Age, Ma	Sm	Nd	$^{147}Sm/^{144}Nd$	$^{143}Nd/^{144}Nd$	$\varepsilon_{Nd}(T)$	T_{Nd}(DM-2st), Ma	Rb	Sr	$^{87}Rb/^{86}Sr$	$(^{87}Sr/^{86}Sr)_{meas}$	$(^{87}Sr/^{86}Sr)_0$	$\varepsilon_{Sr}(T)$
			ppm						ppm					
1	PM-26-11	530	2.761	13.93	0.1198	0.512753±8	+7.5	648	15.1	874	0.04984	0.70412±1	0.7037	–2.0
2	PM-38-11	504	0.911	5.33	0.1033	0.512643±7	+6.1	739	15.6	600	0.07510	0.70413±4	0.7036	–4.6
3	PM-17-11	517	1.805	7.16	0.1524	0.512911±8	+8.3		7.2	715	0.02913	0.70368±2	0.7035	–6.2
4	PM-34-13	521	0.531	2.79	0.1153	0.512776±9	+8.1	585	11.2	526	0.06355	0.70399±6	0.7035	–5.3
5	PM-25-14	495	3.094	14.01	0.1335	0.512443±7	+0.2	1226	22.7	800	0.08224	0.70585±3	0.7053	+19.1
6	PM-23-14	495	0.867	5.74	0.0913	0.512369±10	+1.4	1123	–	–	–	–	–	–
7	PM-31-14	524	3.502	11.69	0.1811	0.512818±8	+4.6	–	21.7	166	0.37692	0.70621±3	0.7034	–7.1
8	PM-28-14	522	3.081	11.97	0.1556	0.512851±9	+6.9	–	25.7	202	0.36885	0.70641±1	0.7037	–3.3
9	PM-62-08	481	0.791	4.00	0.1196	0.512828±11	+8.5	525	7.5	576	0.03759	0.70384±7	0.7036	–5.1

Note. 1, 2, Tugrug pluton (1, diorite–tonalite–plagiogranite association, early phase; 2, plagiogranite association, late phase); 3, Udzur-Hunga pluton (diorite–tonalite–plagiogranite association); 4, Hatan-Hunga pluton (plagiogranite association); 5–6, Mandalt pluton (diorite–tonalite–plagiogranite association); 7, 8, Bayasgalant pluton (7, diorite–tonalite–plagiogranite association, early phase; 8, plagiogranite association, late phase); 9, Dut Uul pluton (plagiogranite association).

ment of their composition points in the Yb–Eu diagram (Table 1, Fig. 2), the rocks melted out from metabasites in equilibrium with the Hbr + CPx + Pl ± Gar restite at ≥10–12 kbar, i.e., probably in the basement of the crust thickened after collision. In contrast to the rocks of the Tugrug and Dut Uul plutons, the plagiogranitoids of the Mandalt pluton are richer in MgO, P_2O_5, Rb, Nb, Ta, Th, U, Hf, V, Cr, Co, and Ni. This suggests a different composition of their mafic magma-generating source enriched in incompatible trace elements. The composition points of these plagiogranitoids fall in the field of OIB in the Y/Nb–Yb/Ta diagram (Fig. 2), which indirectly indicates the relationship of their mafic source with the enriched mantle.

Isotope parameters of the plagiogranitoids and their magma-forming sources

Nd–Sr isotope parameters of the rocks. The island-arc and accretion–collision plagiogranitoids in the south of the Lake Zone show wide variations in isotope parameters (Table 2, Fig. 4) and thus can be divided into two groups, probably formed from different sources. One group includes predominant high- and low-alumina plagiogranitoid associations with ε_{Nd} = 8.5–4.6, T_{Nd}(DM) = 0.7–0.5 Ga, and $(^{87}Sr/^{86}Sr)_0$ = 0.7034–0.7036. High-alumina (adakite-like) plagiogranitoids of this group compose the Tugrug (early and late phases), Udzur-Hunga, Hatan-Hunga, and Dut Uul plutons, and low-alumina plagiogranitoid associations of this group form the early and late phases of the Bayasgalant pluton. Although the low-alumina plagiogranitoids are characterized by lower $\varepsilon_{Nd}(T)$ values than the high-alumina ones, the ranges of the $\varepsilon_{Nd}(T)$ values of these rocks overlap (Table 2, Fig. 4). In general, plagiogranitoid associations with such isotope parameters formed from juvenile sources, which might have been rocks of the "Caledonian" crust of the Lake Zone and/or metabasites of the subducting plate. This follows from the fact that the plagiogranitoids of this group are similar in composition to adakites and their isotope composition points fall in the field of the Lake Zone volcanics in the ε_{Nd}–age diagrams. Another evidence is the arrangement of their composition points near the mantle trend in the ε_{Nd}–ε_{Sr} diagram. In addition, these plagiogranitoids are similar in isotope parameters to the early Paleozoic island-arc and accretion–collision plagiogranitoids in the northern and central parts of the Lake Zone (ε_{Nd} = 9.0–6.6; $(^{87}Sr/^{86}Sr)_0$ = 0.7034–0.7039), which formed from juvenile mafic sources derived from a depleted mantle reservoir (Kovalenko et al., 2004; Kovach et al., 2011; Rudnev et al., 2009, 2013).

The second group includes only the high-alumina plagiogranitoids of the Mandalt pluton, characterized by low ε_{Nd} values (1.4–0.2), a more ancient Nd model age (1.2–1.1 Ga), and $(^{87}Sr/^{86}Sr)_0$ = 0.7053. Plagiogranites with such low $\varepsilon_{Nd}(T)$ values and, obviously, of different genesis have been revealed among early Paleozoic paleogranitoids of the Lake Zone for the first time. Taking into account their geochemical features, melting conditions, and Sr–Nd isotope parameters, we assume that the plagiogranitoid magmas were generated mostly from metabasites formed from an enriched mantle source (e.g., OIB and uplift and plateau basalts).

Note that we have not found early Paleozoic plagiogranitoid associations with lower $\varepsilon_{Nd}(T)$ values and ancient model ages indicating the contribution of ancient Precambrian crustal sources (e.g., the Dzavhan microcontinent rocks) to the generation of granite melts. The absence of this contribution is also evidenced from the age of inherited zircons, 664–531 Ma (Rudnev et al., 2019), corresponding to the formation of the early Cambrian island-arc (~545–520 Ma) and Neoproterozoic ophiolite complexes (Haan Tayshiri, Bayan Nuur, and Bayan Hongor, ~670–560 Ma) of the Lake Zone and adjacent areas.

Hf isotope systematics of magmatic zircons. The early Paleozoic island-arc and accretion–collision plagiogranitoids in the south of the Lake Zone are divided into two groups

Table 3. Lu–Hf isotope composition of zircon (LA-ISP-MS) from plagiogranitoid plutons of the southern Lake Zone

No.	Point	Lu–Hf ratio				$Hf_{initial}$	U–Pb age, Ma	$\varepsilon_{Hf}(T)$	± SE	*T*(DM), Ga	*T*(DM)^{crust}, Ga
		$^{176}Hf/^{177}Hf$	1SE	$^{176}Lu/^{177}Hf$	$^{176}Yb/^{177}Hf$						
Tugrug pluton											
Diorite–tonalite–plagiogranite association, early phase, quartz diorite, sample PM-26-11											
1	1_1	0.282832	0.000007	0.00038	0.014071	0.282828	539	13.5	0.3	0.59	0.62
2	3_1	0.282839	0.000009	0.000460	0.016590	0.282834	534	13.6	0.3	0.58	0.61
3	4_1	0.282837	0.000007	0.001035	0.039825	0.282827	529	13.3	0.2	0.59	0.63
4	5_1	0.282845	0.000007	0.001610	0.062214	0.282829	525	13.3	0.2	0.59	0.63
5	6_1	0.282838	0.000008	0.001044	0.041210	0.282828	531	13.3	0.3	0.59	0.63
6	9_1	0.282833	0.000009	0.000950	0.0359	0.282823	539	13.0	0.3	0.59	0.63
7	10_1	0.282854	0.000006	0.001049	0.041742	0.282843	536	14.0	0.2	0.57	0.59
Plagiogranite association, late phase, plagiogranite, sample PM-38-11											
8	1_1	0.282833	0.000014	0.001600	0.061967	0.282818	512	12.6	0.5	0.60	0.66
9	2_1	0.282815	0.000030	0.003122	0.150251	0.282785	519	11.6	1.1	0.66	0.73
10	3_1	0.282844	0.000022	0.002671	0.121976	0.282819	497	12.3	0.8	0.61	0.67
11	4_1	0.282825	0.000009	0.002656	0.113615	0.282800	495	11.6	0.3	0.63	0.71
12	5_1	0.282775	0.000016	0.004099	0.185945	0.282737	494	9.3	0.6	0.74	0.86
13	6_1	0.282813	0.000021	0.003435	0.155388	0.282780	508	11.2	0.7	0.67	0.75
14	7_1	0.282888	0.000023	0.003307	0.135621	0.282857	504	13.8	0.8	0.55	0.58
15	8_1	0.282841	0.000021	0.002551	0.110958	0.282817	497	12.2	0.7	0.61	0.67
16	4*	0.282874	0.000017	0.002364	0.097648	0.282851	524	14.0	0.6	0.56	0.58
17	6*	0.282531	0.000021	0.001725	0.076166	0.282513	563	2.9	0.7	1.04	1.32
Hatan-Hunga pluton											
Diorite–tonalite–plagiogranite association, quartz diorite, sample PM-34-13											
18	1_1	0.282841	0.000018	0.001226	0.048961	0.282829	517	13.1	0.6	0.59	0.63
19	10_1	0.282879	0.000011	0.001505	0.061863	0.282865	511	14.2	0.4	0.54	0.55
20	2_1	0.282863	0.000010	0.001709	0.066046	0.282846	527	13.9	0.4	0.56	0.59
21	3_1	0.282819	0.000010	0.001170	0.044442	0.282807	531	12.6	0.4	0.62	0.67
22	6_1	0.282825	0.000011	0.001988	0.079916	0.282806	501	11.9	0.4	0.62	0.69
23	7_1	0.282843	0.000011	0.001988	0.081029	0.282824	511	12.8	0.4	0.60	0.65
24	8_1	0.282862	0.000008	0.002087	0.086047	0.282841	528	13.8	0.3	0.57	0.60
25	9_1	0.282853	0.000010	0.000682	0.024066	0.282846	529	14.0	0.3	0.56	0.58
26	1*	0.282678	0.000028	0.004673	0.17501	0.282630	545	6.7	1.0	0.90	1.07
27	11*	0.28268	0.000031	0.001048	0.036287	0.282667	664	10.6	1.1	0.81	0.91
Mandalt pluton											
Diorite–tonalite–plagiogranite association, quartz diorite, sample PM-25-14											
28	6	0.282695	0.000016	0.002063	0.081611	0.282676	496	7.2	0.6	0.81	0.99
29	9	0.282679	0.000014	0.002995	0.126419	0.282651	495	6.3	0.5	0.86	1.05
30	10	0.282649	0.000017	0.002386	0.102548	0.282627	495	5.4	0.6	0.89	1.10
31	20	0.282648	0.000019	0.00219	0.086309	0.282628	498	5.5	0.7	0.88	1.10
32	29	0.282665	0.000015	0.002802	0.12001	0.282639	489	5.7	0.5	0.87	1.08
33	30	0.282667	0.000016	0.001653	0.068401	0.282652	486	6.1	0.6	0.84	1.05
34	44	0.282651	0.000020	0.002157	0.088437	0.282631	490	5.5	0.7	0.88	1.10
35	47C	0.282696	0.000022	0.002838	0.110018	0.282670	489	6.8	0.8	0.83	1.01
36	7*	0.282872	0.000024	0.002985	0.105791	0.282843	519	13.6	0.8	0.57	0.60
37	14*	0.282855	0.000014	0.002175	0.084230	0.282833	530	13.5	0.5	0.58	0.61
38	28C*	0.282869	0.000012	0.002276	0.090088	0.282847	525	13.9	0.4	0.56	0.59
39	28R*	0.282857	0.000010	0.001513	0.057713	0.282842	520	13.6	0.4	0.57	0.60

Table 3 (*continued*)

No.	Point	Lu–Hf ratio				$Hf_{initial}$	U–Pb age, Ma	$\varepsilon_{Hf}(T)$	± SE	*T*(DM), Ga	*T*(DM)^{crust}, Ga
		$^{176}Hf/^{177}Hf$	1SE	$^{176}Lu/^{177}Hf$	$^{176}Yb/^{177}Hf$						
Bayasgalant pluton Tonalite–plagiogranite association, early phase, tonalite, sample PM-31-14											
40	1	0.282832	0.000010	0.002023	0.081783	0.282812	527	12.7	0.3	0.61	0.66
41	2	0.282836	0.000011	0.002905	0.119927	0.282808	522	12.4	0.4	0.62	0.68
42	14R	0.282885	0.000011	0.001711	0.069563	0.242868	523	14.6	0.4	0.53	0.54
43	17	0.282856	0.000019	0.001553	0.062645	0.282841	523	13.6	0.7	0.57	0.60
44	20	0.282849	0.000014	0.001732	0.063166	0.282832	528	13.4	0.5	0.58	0.62
45	22	0.282826	0.000009	0.001844	0.072787	0.282808	527	12.6	0.3	0.62	0.67
46	23	0.282879	0.000009	0.002081	0.085800	0.282859	522	14.2	0.3	0.54	0.56
47	24	0.282846	0.000016	0.002239	0.088423	0.282824	521	13.0	0.6	0.60	0.64
48	25R	0.282838	0.000013	0.002280	0.090936	0.282816	525	12.8	0.5	0.61	0.66
49	30C	0.282829	0.000015	0.002635	0.103288	0.282803	525	12.3	0.5	0.63	0.69
50	34	0.282845	0.000010	0.002019	0.078544	0.282825	525	13.1	0.4	0.59	0.63
51	42	0.282878	0.000011	0.002346	0.094866	0.282855	528	14.2	0.4	0.55	0.57
52	48	0.282911	0.000012	0.002359	0.095548	0.282888	521	15.3	0.4	0.50	0.50
53	26C*	0.282871	0.000010	0.001855	0.071511	0.282852	537	14.3	0.4	0.55	0.57
54	35C*	0.282884	0.000013	0.001948	0.080363	0.282864	535	14.7	0.5	0.54	0.54
55	44*	0.282854	0.000011	0.001898	0.073978	0.282835	538	13.8	0.4	0.58	0.60
56	51*	0.282865	0.000014	0.001946	0.078417	0.282845	539	14.2	0.5	0.56	0.58
57	52*	0.282882	0.000015	0.001965	0.080692	0.282862	536	14.7	0.5	0.54	0.54
Plagiogranite association, late phase, plagiogranite, sample PM-28-14											
58	2R	0.282874	0.000009	0.001743	0.066531	0.282857	520	14.1	0.3	0.55	0.57
59	3R	0.282851	0.000008	0.001882	0.073573	0.282833	523	13.3	0.3	0.58	0.62
60	4C	0.282865	0.000012	0.002035	0.071724	0.282845	515	13.7	0.4	0.56	0.60
61	5	0.282885	0.000011	0.001884	0.071449	0.282866	524	14.6	0.4	0.53	0.54
62	8C	0.282839	0.000010	0.002708	0.105087	0.282813	521	12.6	0.4	0.61	0.67
63	11C	0.28287	0.000009	0.002799	0.111326	0.282843	519	13.6	0.4	0.57	0.60
64	12C	0.282854	0.000011	0.002312	0.089169	0.282831	526	13.4	0.4	0.59	0.62
65	13C	0.282846	0.000009	0.002173	0.084285	0.282825	520	13.0	0.3	0.59	0.64
66	17	0.282851	0.000010	0.002069	0.082588	0.282831	519	13.2	0.4	0.59	0.63
67	20	0.28287	0.000009	0.001730	0.063929	0.282853	525	14.1	0.4	0.55	0.57
68	21	0.282854	0.000011	0.002062	0.077746	0.282834	523	13.4	0.4	0.58	0.62
69	23C	0.282873	0.000014	0.002136	0.087301	0.282852	521	14.0	0.5	0.55	0.58
70	25	0.282854	0.000010	0.002707	0.10281	0.282827	528	13.3	0.4	0.59	0.63
71	27	0.282873	0.000010	0.001494	0.056631	0.282858	526	14.3	0.4	0.54	0.56
72	34	0.282846	0.000010	0.001833	0.070747	0.282828	523	13.2	0.4	0.59	0.63
73	2C*	0.282837	0.000012	0.002762	0.111405	0.282809	535	12.8	0.4	0.62	0.66
74	4R*	0.282871	0.000011	0.001620	0.056146	0.282855	538	14.5	0.4	0.55	0.56
75	12R*	0.282852	0.000009	0.002018	0.076985	0.282832	535	13.6	0.3	0.58	0.61
Dut Uul pluton Plagiogranite association, plagiogranite, sample PM-62-08											
76	1_1	0.282833	0.000011	0.003345	0.142074	0.282802	488	11.5	0.4	0.63	0.71
77	3_1	0.282892	0.000012	0.001059	0.037891	0.282882	492	14.4	0.4	0.51	0.53
78	4_1	0.282865	0.000014	0.001695	0.066706	0.282849	506	13.5	0.5	0.56	0.59
79	4_2	0.282885	0.000010	0.001961	0.083739	0.282868	475	13.5	0.4	0.53	0.57
80	5_1	0.282864	0.000012	0.002443	0.108474	0.282842	487	12.9	0.4	0.57	0.62

Table 3 (*continued*)

No.	Point	Lu–Hf ratio				$Hf_{initial}$	U–Pb age, Ma	$\varepsilon_{Hf}(T)$	± SE	*T*(DM), Ga	$T(DM)^{crust}$, Ga
		$^{176}Hf/^{177}Hf$	1SE	$^{176}Lu/^{177}Hf$	$^{176}Yb/^{177}Hf$						
81	6_1	0.28286	0.000014	0.001430	0.056881	0.282847	490	13.1	0.5	0.56	0.61
82	9_1	0.282897	0.000022	0.001323	0.055181	0.282865	477	14.2	0.8	0.51	0.53
83	2*	0.282849	0.000012	0.001540	0.063003	0.282833	540	13.8	0.4	0.58	0.61

Note. C, core, R, rim. A Hf isotope study of zircons (Fig. 7) was carried out at the same local points as the earlier U–Pb isotope study (Rudnev et al., 2019). *Points where isotope measurements were made for xenogenic/inherited zircons; the rest are the points of measurements for magmatic zircons.

according to Hf isotope composition, which correspond to the groups recognized from Nd–Sr isotope parameters.

The first (main) group comprises the rocks of island-arc plagiogranitoid associations (Tugrug, Hatan-Hunga, and Bayasgalant plutons) containing magmatic zircons with a narrow range of ε_{Hf} values (14.7–11.9) and late Neoproterozoic model ages (0.7–0.5 Ga; Table 3, Fig. 6). This group includes plagiogranites of the Tugrug (late phase) and Dut Uul plutons, which formed at the accretion–collision stage. Magmatic zircons from these plutons have a wider range of isotope parameter values ($\varepsilon_{Hf}(T)$ = 14.2–9.3 and $T(DM)^{crust}$ = 0.9–0.5 Ga; Table 3, Fig. 6), which largely overlap with the values of zircons from island-arc plagiogranitoids. The similar isotope characteristics of magmatic zircons and the similar Nd isotope parameters of plagiogranitoids differing in composition (high- and low-alumina) and formation conditions suggest that the rocks formed from metabasic sources of similar compositions and ages derived from the depleted mantle.

The second group is the high-alumina plagiogranitoids of the Mandalt pluton. The hosted zircons are characterized by much lower $\varepsilon_{Hf}(T)$ values (7.2–5.4) and older model ages (1.1–1.0 Ga). In the $\varepsilon_{Hf}(T)$–age diagram they form an individual field (Fig. 6). The lower $\varepsilon_{Hf}(T)$ values of magmatic zircons are correlated with the lower $\varepsilon_{Nd}(T)$ and higher $(^{87}Sr/^{86}Sr)_0$ values of these plagiogranitoids. This, along with the rock composition (Table 1, Figs. 2 and 3), suggests that the parental melts for the Mandalt pluton were generated primarily from metabasites formed either from a weakly depleted mantle source or from both enriched and depleted sources.

The magmatic zircons from the studied plagiogranitoids overlap in Hf isotope parameters with the zircons from island-arc plagiogranitoid associations (560–510 Ma) of the central and northern Lake Zone ($\varepsilon_{Hf}(T)$ = 16.5–11.2, $T(DM)^{crust}$ = 0.9–0.5 Ga) (Kovach et al., 2017) and with the magmatic zircons from gabbroid and granitoid associations (538–494 Ma) found south of the Altay aimak (Haan Tayshiri intrusive area, Fig. 1), on the southern slopes of the Haan Tayshiri Range ($\varepsilon_{Hf}(T)$ = 14.3–2.5, $T(DM)^{crust}$ = 1.3–0.5 Ga) (Janoušek et al., 2018).

Hf isotope systematics of inherited and xenogenic zircons. Based on the results of U–Pb isotope studies of inherited and xenogenic zircons from plagiogranitoids, we divided them into four age groups: ~664, 570–560, 545–531, and 530–519 Ma (Rudnev et al., 2018, 2019). According to the Lu–Hf isotope parameters, we recognized three groups of these zircons.

The first (main) group comprises predominant inherited zircons (540–524 Ma) and scarce xenogenic zircons (530–519 Ma). Inherited zircons are found in the island-arc plagiogranitoids of the Bayasgalant pluton (539–535 Ma) and in the late-phase accretion–collision plagiogranites of the Tugrug (~524 Ma; Table 3, Fig. 6) and Dut Uul (~540 Ma) plutons. They are characterized by a narrow range of isotope parameters ($\varepsilon_{Hf}(T)$ = 14.5–12.8) and late Neoproterozoic model ages (0.7–0.5 Ga) and do not differ from the magmatic zircons of the first group in the same rocks ($\varepsilon_{Hf}(T)$ = 14.7–11.9). Note that the similar isotope parameters of inherited and magmatic zircons suggest their formation from the sources of similar compositions and ages. Judging from the time of the formation of inherited zircons and their CL images indicating their magmatic origin, these zircons crystallized in the igneous rocks of early Cambrian island-arc complexes (granitoids, gabbroids, and volcanics).

This isotope group also includes xenogenic zircons from the rocks of the Mandalt pluton (530–519 Ma), similar in isotope parameters (530–519 Ma) to the above inherited zircons. As established earlier, these xenogenic zircons lack traces of dissolution and overgrowth with magmatic zircons of later generation (Rudnev et al., 2019). Therefore, we assume that they were borrowed by granitoid melt from the host rocks (early Cambrian volcanics) at the depth of its formation. Most likely, the estimated isotope parameters reflect the isotope composition of the source of the host volcanics.

The isotope data on the inherited zircons of the second and third groups are scarce and, therefore, permit only preliminary conclusions. Nevertheless, they show that the sources of different ages and compositions that formed at the island-arc and accretion–collision stages of the regional evolution were involved in the formation of parental melts that produced plagiogranitoids in the south of the Lake Zone. The second group includes inherited zircons (~563 Ma) from the late-phase plagiogranitoids of the Tugrug pluton, with ε_{Hf} = 2.9 and a model age of 1.3 Ga. Zircons with such isotope parameters have been found in granitoids of early Paleozoic age for the first time; therefore, it is still premature to draw conclusions about their sources. Taking

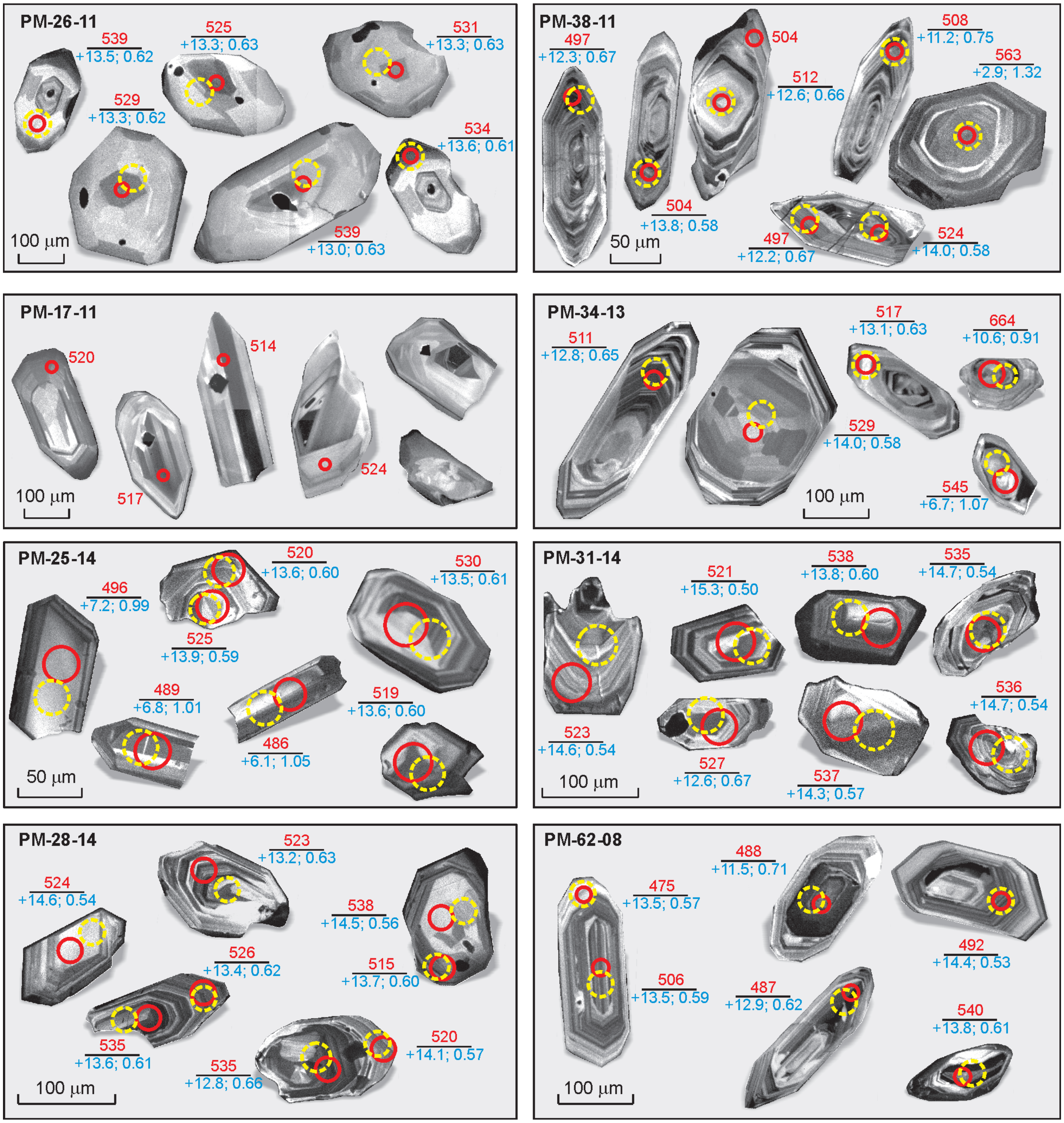

Fig. 5. Cathodoluminescence (CL) images of zircon grains from plagiogranitoids of the southern Lake Zone. Red circles mark the points of U–Pb isotope studies of magmatic and xenogenic zircons (Rudnev et al., 2019), and yellow circles, the points of their Lu–Hf isotope studies (Table 3). Above the line—age, Ma, below the line—ε_{Hf} values and $T(DM)^{crust}$, Ga. Tugrug pluton: sample PM-26-11 (quartz diorite) and sample PM-38-11 (plagiogranite); Udzur-Hunga pluton—sample PM-17-11 (quartz diorite); Hatan-Hunga pluton—sample PM-34-13 (plagiogranite); Mandalt pluton—sample PM-25-14 (quartz diorite); Bayasgalant pluton—sample PM-31-14 (plagiogranite) and sample PM-28-14 (plagiogranite); Dut Uul pluton—sample PM-62-08 (plagiogranite).

into account the magmatic nature and age of these inherited zircons and the geologic structure of geoblocks adjacent to the Lake Zone (Fig. 1), we can assume that they might have formed from products of destruction and erosion of igneous rocks (gabbroids and plagiogranitoids) of ophiolite complexes of close ages (Haan Tayshiri, 573–565 Ma; Baya Nuur, 565–560 Ma; and Bayan Hongor, 577–569 Ma) (Gibsher et al., 2001; Buchan et al., 2002; Kozakov et al., 2002; Terent'eva et al., 2010; Yarmolyuk et al., 2011; Jian et al., 2014). To check this assumption, it is necessary to carry out additional Lu–Hf isotope studies of zircons from rocks of ophiolite complexes of the same age located near the studied early Paleozoic plagiogranitoid associations of the southern Lake Zone (in particular, the Bayan Nuur complex of the

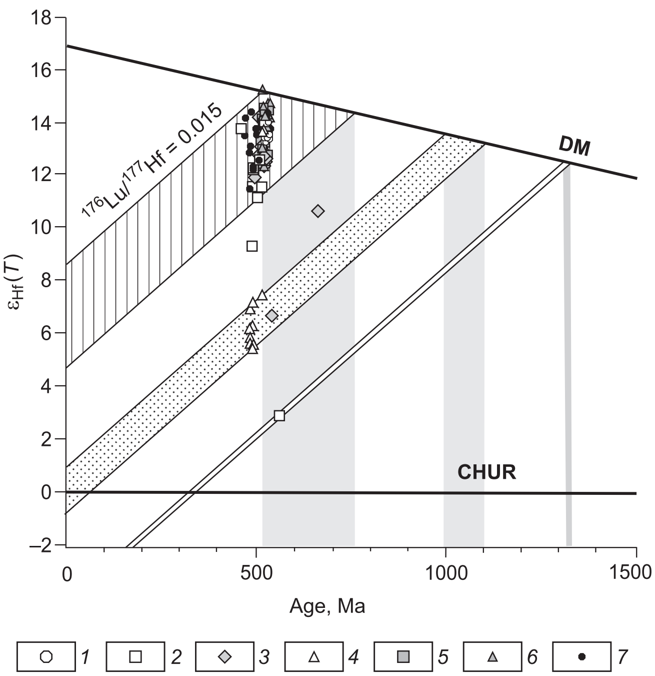

Fig. 6. ε_{Hf}–age diagram for zircons from early Paleozoic plagiogranitoids of the southern Lake Zone (Table 3). Designations follow Fig. 2.

Dariv Range and the Haan Tayshiri complex of the Haan Tayshiri Range).

The third group unites inherited zircons of different ages (~545 and 664 Ma (Rudnev et al., 2019)) from the island-arc high-alumina plagiogranites of the Hatan-Hunga pluton. In Hf isotope parameters ($\varepsilon_{Hf}(545)$ = 6.7 and $\varepsilon_{Hf}(664)$ = 10.6) they are intermediate between the zircons of the first and second groups. These isotope parameters suggest that the inherited zircons of two ages resulted from the melting of metabasites of depleted mantle sources, but a definite conclusion about their origin requires additional geochronological and isotope studies. We can only assume that these zircons formed in sediments resulted from the destruction and erosion of late Neoproterozoic island-arc rocks (granitoids, gabbroids, and volcanics) and Neoproterozoic ophiolite complexes (e.g., the Bayan Hongor one). We need additional geological, geochronological, and isotope studies to confirm this assumption.

Note that we have not found older inherited zircons with lower values of Hf isotope parameters indicating the presence of ancient crustal substrates (e.g., the Dzavhan microcontinent). This fact apparently indicates that the island arc of the Lake Zone is far from ancient Precambrian blocks (microcontinents), at least those dated at 530–485 Ma.

CONCLUSIONS

(1) According to their petrochemical and trace-element compositions, the early Paleozoic plagiogranitoid associations of the island-arc (531–517 Ma) and accretion–collision (504–481 Ma) stages are of the high- and low-alumina types. High-alumina rocks (Tugrug, Hatan-Hunga, and Udzur-Hunga plutons) are the most widespread among the island-arc plagiogranitoid associations (531–517 Ma), which are similar in trace-element composition to high-silica adakites. They resulted, most likely, from the partial melting of MORB-type metabasites in equilibrium with the garnet-containing restite at ≥10–12 kbar during the subduction of oceanic plate. The rocks of the Bayasgalant pluton (524–522 Ma) are low-alumina plagiogranites. Their parental melts formed through the melting of metabasites localized in the basement of an island-arc system in equilibrium with plagioclase-containing restite at ≤8 kbar. According to their petrogeochemical characteristics, the accretion–collision plagiogranitoid associations in the south of the Lake Zone (Tugrug, Mandalt, and Dut Uul plutons) are of high-alumina type and formed through the melting of metabasites in equilibrium with garnet-bearing restite in the basement of thick crust at ≥10–12 kbar.

(2) The obtained Sr–Nd isotope data have revealed two groups of plagiogranitoid associations of the southern Lake Zone, reflecting different sources of their parental melts. The first group includes most of plagiogranitoid associations formed at the island-arc (Tugrug, Udzur-Hunga, Hatan-Hunga, and Bayasgalant plutons) and accretion–collision (Tugrug and Dut Uul plutons) stages of the regional evolution, with isotope parameters ε_{Nd} = 8.5–4.6 and $(^{87}Sr/^{86}Sr)_0$ = 0.7034–0.7036 indicating primarily the juvenile sources. The same is also evidenced by the similarity of the plagiogranitoids of this group to adakites and by the arrangement of their isotope composition points in the Nd isotope composition field of the Lake Zone volcanics. The second group is only the Mandalt pluton plagiogranitoids with ε_{Nd} = 1.4–0.2 and $(^{87}Sr/^{86}Sr)_0$ = 0.7053. The Sr–Nd isotope parameters of these rocks, along with their trace-element composition, suggest that the parental melts formed mostly from metabasites derived from an enriched mantle source.

(3) The Hf isotope studies have revealed two groups of magmatic zircons in the rocks of the studied plagiogranitoid associations. The first group includes magmatic zircons from the plagiogranitoids of the Tugrug, Hatan-Hunga, Bayasgalant, and Dut Uul plutons with high positive ε_{Hf} values (14.7–11.9) indicating the depleted composition of their magma-forming sources. The second group is zircons from the plagiogranitoids of the Mandalt pluton with isotope parameters $\varepsilon_{Hf}(T)$ = 7.2–5.4, which suggests melting of a basic substrate (oceanic uplifts, plateaus, and islands) derived from a relatively enriched mantle source. Thus, the Hf isotope characteristics of magmatic zircons and the Sm–Nd isotope parameters of the host rocks indicate an inhomogeneous composition of the magma-generating sources of the plagiogranitoids and a heterogeneous composition of the crust in the Lake Zone of Western Mongolia.

(4) The Hf isotope studies have revealed three groups of inherited and xenogenic zircons (664–519 Ma) in the early Paleozoic plagiogranitoid associations of the southern Lake

Zone. The first group includes inherited and xenogenic zircons with ages of 540–519 Ma and ε_{Hf} = 14.5–12.8 found in the rocks of the Bayasgalant, Tugrug, Dut Uul, and Mandalt plutons. According to the isotope data, they do not differ from the magmatic zircons of these rocks, which indicates predominantly early Cambrian magma-forming sources of similar composition and age. The second and third groups include single grains of inherited zircons from the rocks of the Tugrug and Hatan-Hunga plutons, which show lower values of isotope parameters (ε_{Hf}(563) = 2.9, ε_{Hf}(545) = 6.7, and ε_{Hf}(664) = 10.6). This suggests a less depleted composition and/or more ancient age of their sources.

(5) The Rb–Sr, Sm–Nd, and Lu–Hf isotope data show that the parental melts for the early Paleozoic plagiogranitoids of the southern Lake Zone formed far from early Precambrian blocks having a longer crustal history, such as the Dzavhan and other microcontinents.

We are deeply grateful to O.M. Turkina, A.E. Izokh, and N.N. Kruk for fruitful discussions and valuable advice and comments on the manuscript, reviewer T.V. Donskaya and the anonymous reviewer for valuable critical remarks, E.A. Kruk (V.S. Sobolev Institute of Geology and Mineralogy SB RAS, Novosibirsk) for treatment of stone materials and processing of maps, and S.V. Palesskii, G.A. Dokukina, N.G. Karmanova, A.N. Toryanik, and N.M. Glukhova (V.S. Sobolev Institute of Geology and Mineralogy SB RAS, Novosibirsk) for analyses.

The work is done on state assignment of the V.S. Sobolev Institute of Geology and Mineralogy, SB RAS, and with financial support by grants 18-05-00105a and 15-05-05615a from the Russian Foundation for Basic Research.

REFERENCES

Arth, J.G., 1979. Some trace elements in trondhjemites. Their implications to magma genesis and paleotectonic setting, in: Barker, F. (Ed.), Trondhjemites, Dacites and Related Rocks. Elsevier, Amsterdam, pp. 123–132.

Badarch, G., Cunningham, W.D., Windley, B.F., 2002. A new terrane subdivision for Mongolia: Implications for the Phanerozoic crustal growth of Central Asia. J. Asian Earth Sci. 21, 87–104.

Beard, J.S., Lofgren, G.E., 1991. Dehydration melting and water-saturated melting of basaltic and andesitic greenstones and amphibolites at 1, 3 and 6.9 kbar. J. Petrol. 32, 365–401.

Buchan, C., Pfänder, J., Kröner, A., Brewer, T.S., Tomurtogoo, O., Tomurhuu, D., Cunningham, D., Windley, B.F., 2002. Timing of accretion and collisional deformation in the Central Asian Orogenic Belt: implications of granite geochronology in the Bayankhongor Ophiolite Zone. Chem. Geol. 192, 23–45.

Castillo, P.R., 2006. An overview of adakite petrogenesis. Chinese Sci. Bull. 51 (3), 257–268.

Dergunov, A.B., 1989. The Caledonides of Central Asia. Transactions of the Geological [in Russian]. Nauka, Moscow, pp. 1–192.

Dergunov, A.B., Kovalenko, V.I., Ruzhentsev, S.V., Yarmolyuk, V.V., 2001. Tectonic, Magmatism, and Metallogeny of Mongolia. Routledge, London, New York.

Eby, G.N., 1990. The *A*-type granitoids: A review of their occurrence and chemical characteristics and speculation on their petrogenesis. Lithos 26, 115–134.

Gibsher, A.S., Khain, E.V., Kotov, A.B., Sal'nikova, E.B., Kozakov, I.K., Kovach, V.P., Yakovleva, S.Z., Fedoseenko, A.M., 2001. Late Vendian age of the Han-Taishiri ophiolite complex in western Mongolia. Russian Geology and Geophysics (Geologiya i Geofizika) 42 (8), 1179–1185 (1110–1117).

Goldstein, S.J., Jacobsen, S.B., 1988. Nd and Sr isotopic systematics of river water suspended material: Implications for crustal evolution. Earth Planet. Sci. Lett. 87, 249–265.

Griffin, W.L., Pearson, N.J., Belousova, E.A., Jackson, S.R., van Achterbergh, E., O'Reilly, S.Y., Shee, S.R., 2000. The Hf isotope composition of cratonic mantle: LAM-MC-ICP MS analysis of zircon megacrysts in kimberlites. Geochim. Cosmochim. Acta 64, 133–147.

Griffin, W.L., Belousova, E.A., Shee, S.R., Pearson, N.J., O'Reilly, S.Y., 2004. Archean crustal evolution in the northern Yilgarn Craton: U–Pb and Hf-isotope evidence from detrital zircons. Precambrian Res. 131, 231–282.

Jacobsen, S.B., Wesserburg, G.J., 1984. Sm–Nd evolution of chondrites and achondrites. Earth Planet. Sci. Lett. 67, 137–150.

Jahn, B.M., 2004. The Central Asian Orogenic Belt and growth of the continental crust in the Phanerozoic, in: Malpas, J., Fletcher, C.J.N., Aitchison, J.C. (Eds.), Aspects of the Tectonic Evolution of China. Geol. Soc. London, Spec. Publ. 226, 73–100.

Jahn, B.M., Wu, F., Chen, B., 2000a. Granitoids of the Central Asian Orogenic Belt and continental growth in the Phanerozoic. Trans. R. Soc. Edinburgh 91, 181–193.

Jahn, B.M., Wu, F., Chen, B., 2000b. Massive granitoid generation in Central Asia: Nd isotope evidence and implication for continental growth in the Phanerozoic. Episodes 23, 82–92.

Janoušek, V., Jiang, Y., Buriánek, D., Schulmann, K., Hanžl, P., Soejono, I., Kröner, A., Altanbaatar, B., Erban, V., Lexa, O., Ganchuluun, T., Košler, J., 2018. Cambrian–Ordovician magmatism of the Ikh-Mongol Arc System exemplified by the Khantaishir Magmatic Complex (Lake Zone, south-central Mongolia). Gondwana Res. 54, 122–149.

Jian, P., Kröner, A., Jahn, B.-M., Windley, B.F., Shi, Y., Zhang, W., Zhang, F., Miao, L., Tomurhuu, D., Liu, D., 2014. Zircon dating of Neoproterozoic and Cambrian ophiolites in West Mongolia and implications for the timing of orogenic processes in the central part of the Central Asian Orogenic Belt. Earth Sci. Rev. 133, 62–93.

Kovach, V.P., Yarmolyuk, V.V., Kovalenko, V.I., Kozlovskyi, A.M., Kotov, A.B., Terent'eva, L.B., 2011. Composition, sources, and mechanisms of formation of the continental crust of the Lake Zone of the Central Asian Caledonides. II. Geochemical and Nd isotope data. Petrology 19 (4), 399–425.

Kovach, V.P., Rudnev, S.N., Kruk, N., Yarmolyuk, V., Wang, K.L., Kotov, A., Chung, S.L., 2017. Latest Neoproterozoic–early Paleozoic juvenile crust growth in the central part of the Central Asian Orogenic Belt: Insight from Nd–Hf isotopic data for the Altai–Sayan–Western Mongolia region, in: Asian Orogeny and Continental Evolution: New Advances from Geologic, Geophysical and Geochemical Perspectives. International Conference in Memory of Prof. Bor-ming Jahn, Taipei, Taiwan, November 6–7, 2017. Academia Sinica, Taipei, pp. 48–50.

Kovalenko, V.I., Yarmolyuk, V.V., Sal'nikova, E.B., Kartashov, P.M., Kovach, V.P., Kozakov, I.K., Kozlovskii, A.M., Kotov, A.B., Ponomarchuk, V.A., Listratova, E.N., Yakovleva, S.Z., 2004. The Khaldzan–Buregtei massif of peralkaline rare-metal igneous rocks: structure, geochronology, and geodynamic setting in the Caledonides of Western Mongolia. Petrology 12 (5), 412–436.

Kozakov, I.K., Sal'nikova, E.B., Khain, E.V., Kovach, V.P., Berezhnaya, N.G., Yakovleva, S.Z., Plotkina, Yu.V., 2002. Early Caledonian crystalline rocks of the Lake Zone in Mongolia: formation history and tectonic settings as deduced from U–Pb and Sm–Nd datings. Geotectonics 36 (2), 156–166.

Kröner, A., Kovach, V., Belousova, E., Hegner, E., Amstrong, R., Dolgopolova, A., Seltmann, R., Alexeiev, D.V., Hoffmann, J.E., Wong, J., Sun, M., Cai, K., Wang, T., Tong, Y., Wilde, S.A., Degtyarev, K.E., Rytsk, E., 2014. Reassessment of continental growth during the accretionary history of the Central Asian Orogenic Belt. Gondwana Res. 25, 103–125.

Liew, T.C., Hofmann, A.W., 1988. Precambrian crustal components, plutonic associations, plate environment of the Hercynian Fold Belt of central Europe: Indications from a Nd and Sr isotopic study. Contrib. Mineral. Petrol. 98, 129–138.

Martin, H., Smithies, R.H., Rapp, R., Moyen, J.F., Champion, D., 2005. An overview of adakite, tonalite–trondhjemite–granodiorite (TTG), and sanukitoid: relationships and some implication for crustal evolution. Lithos 79, 1–24.

Nikolaeva, I.V., Palesskii, S.V., Koz'menko, O.A., Anoshin, G.N., 2008. Analysis of geologic reference materials for REE and HFSE by inductively coupled plasma–mass spectrometry (ICP-MS). Geochem. Int. 46 (10), 1016–1022.

Pearce, J.A., Harris, N.B.W., Tindle, A.G., 1984. Trace element discrimination diagrams for the tectonic interpretation of granitic rocks. J. Petrol. 25, 956–983.

Pearson, N.J., Griffin, W.L., O'Reilly, S.Y., 2008. Precision of in situ isotope ratio measurements by LAM-MC-ICPMS. Geochim. Cosmochim. Acta 72, A732.

Rapp, R.P., Watson, E.B., 1995. Dehydration melting of metabasalt at 8–32 kbar: implications for continental growth and crust–mantle recycling. J. Petrol. 36, 891–931.

Rapp, R.P., Watson, E.B., Miller, C.F., 1991. Partial melting of amphibolite/eclogite and the origin of Archean trondhjemites and tonalities. Precambrian Res. 151, 1–25.

Rudnev, S.N., Izokh, A.E., Kovach, V.P., Shelepaev, R.A., Terent'eva, L.B., 2009. Age, composition, sources, and geodynamic environments of the origin of granitoids in the northern part of the Ozernaya Zone, Western Mongolia: growth mechanisms of the Paleozoic continental crust. Petrology 17 (5), 439–475.

Rudnev, S.N., Izokh, A.E., Borisenko, A.S., Shelepaev, R.A., Orihashi, Y., Lobanov, K.V., Vishnevsky, A.V., 2012. Early Paleozoic magmatism in the Bumbat–Hairhan area of the Lake Zone in western Mongolia (geological, petrochemical, and geochronological data). Russian Geology and Geophysics (Geologiya i Geofizika) 53 (5), 425–441 (557–578).

Rudnev, S.N., Kovach, V.P., Ponomarchuk, V.A., 2013. Vendian–Early Cambrian island-arc plagiogranitoid magmatism in the Altai–Sayan folded area and in the Lake Zone of western Mongolia (geochronological, geochemical, and isotope data). Russian Geology and Geophysics (Geologiya i Geofizika) 54 (10), 1272–1287 (1628–1647).

Rudnev, S.N., Izokh, A.E., Borisenko, A.S., Gas'kov, I.V., 2016. Granitoid magmatism and metallogeny of the Lake Zone in Western Mongolia (by the example of the Bumbat-Hairhan area). Russian Geology and Geophysics (Geologiya i Geofizika) 57 (2), 207–224 (265–286).

Rudnev, S.N., Mal'kovets, V.G., Belousova, E.A., Tret'yakova, I.G., Gibsher, A.A., 2018. U–Pb isotope dating of xenogenic zircon from early Paleozoic plagiogranitoids of the southern part of the Lake Zone in Mongolia, in: Methods and Geological Results of Study of Geochronometric Isotope Systems of Minerals and Rocks. Proceedings of the Seventh Russian Conference on Isotope Geochronology [in Russian]. IGEM RAN, Moscow, pp. 294–296.

Rudnev, S.N., Mal'kovets, V.G., Belousova, E.A., Tret'yakova, I.G., Gibsher, A.A., 2019. Composition and age of plagiogranitoids in the south of the Lake Zone (*Western Mongolia*). Russian Geology and Geophysics (Geologiya i Geofizika) 60 (11), 1205–1228 (1513–1541).

Scherer, E., Münker, C., Mezger, K., 2001. Calibration of the Lutetium–Hafnium clock. Science 293 (5530), 683–687

Sun, S.S., McDonough, W.F., 1989. Chemical and isotopic systematics of oceanic basalts: Implications for mantle composition and processes, in: Saunders, A.D., Norry, M. (Eds.), Magmatism in the Ocean Basins. Geol. Soc. London, Spec. Publ. 42, 313–345.

Taylor, S.R., McLennan, S.M., 1985. The Continental Crust: Its Evolution and Composition. Blackwell, London.

Terent'eva, L.B., Kozakov, I.K., Yarmolyuk, V.V., Anisimova, I.V., Kovach, V.P., Kozlovskii, A.M., Kudryashova, E.A., Sal'nikova, E.B., Yakovleva, S.Z., Fedoseenko, A.M., Plotkina, Yu.V., 2010. Convergent processes in the evolution of the early Caledonian Bayan-Khongor zone of Central Asia: Evidence from geological and geochronological investigations of the Khan-Ula gabbroid pluton. Dokl. Earth Sci. 433 (1), 937–943.

Tomurtogoo, O. (Ed.), 1999. Geological Map of Mongolia. General Directorate of Mineral Research and Exploration of Turkey. Ankara.

Turkina, O.M., 2000. Modeling geochemical types of tonalite–trondhjemite melts and their natural equivalents. Geochem. Int. 38 (7), 640–651.

Yarmolyuk, V.V., Kovach, V.P., Kovalenko, V.I., Salnikova, E.B., Kozlovskii, A.M., Kotov, A.B., Yakovleva, S.Z., Fedoseenko, A.M., 2011. Composition, sources, and mechanism of continental crust growth in the Lake Zone of the Central Asian Caledonides: I. Geological and geochronological data. Petrology 19 (1), 55–78.

Yarmolyuk, V.V., Kovach, V.P., Kozakov, I.K., Kozlovsky, A.M., Kotov, A.B., Rytsk, E.Yu., 2012. Mechanisms of continental crust formation in the Central Asian Foldbelt. Geotectonics 46 (4), 251–272.

Editorial responsibility: O.M. Turkina